クロマグロの性分化制御機構に関する研究

Doctoral Dissertation

STUDIES ON SEX DIFFERENTIATION IN PACIFIC BLUEFIN TUNA *Thunnus orientalis*

March 2024

Graduate School of Marine Science and Technology

Tokyo University of Marine Science and Technology

Doctoral Course of Applied Marine Biosciences

HAYASHIDA TAKAO

Doctoral Dissertation

STUDIES ON SEX DIFFERENTIATION IN PACIFIC BLUEFIN TUNA *Thunnus orientalis*

March 2024

Graduate School of Marine Science and Technology

Tokyo University of Marine Science and Technology

Doctoral Course of Applied Marine Biosciences

HAYASHIDA TAKAO

Contents

Acknowledgments

I would first like to express my gratitude and appreciation to Professor Yukinori Kazeto, Glass Eel Production Division of the Fisheries Technology Institute for all his support.

I thank Prof. Motohiko Sano of the Laboratory of Fish Pathology, Course of Applied Marine Biosciences, Graduate School of Marine Science and Technology, Tokyo University of Marine Science and Technology, Associate Prof. Yuichi Ozaki of the Laboratory of Physiological Function, Division of Aquaculture Research, Department of Fisheries Technology Institute, and Associate Prof. Yutaka Haga of the Laboratory of Fish Nutrition, Course of Applied Marine Biosciences, Graduate School of Marine Science and Technology, Tokyo University of Marine Science and Technology for critical reading of the manuscript.

I would also like to extend my appreciation to all staff members of Tuna Aquaculture Division, Fisheries Technology Institute, for their assistance with the maintenance and sampling of the fish in this study.

Chapter 1.

General Introduction

Tunas (*Thunnus* spp.) are widely distributed in the global ocean and are top predators in marine ecosystems. Tuna, specifically bluefin tuna, has a high market demand and value; therefore, tuna is of substantial commercial interest to fisheries and aquaculture operations worldwide. Although tuna fishing has been practiced for several millennia, tuna aquaculture is a relatively new industry (Benetti et al., 2016). Although early tuna aquaculture efforts date back to the late 1960s, it was not until the early 1990s that industrial-scale farming developed into the modern industry (Benetti et al., 2016).

Pacific bluefin tuna (*T. orientalis*; hereafter, PBT) is one of the most important species for aquaculture worldwide (Masuma et al., 2011). Owing to the global increase in the supply of bluefin tuna species for human consumption, bluefin tuna aquaculture has been expanded and widely undertaken in many countries, including Mexico, Australia, Japan, and the Mediterranean Sea (Masuma et al., 2011). However, fish for breeding bluefin tuna species in aquaculture have been largely sourced from wild-caught fingerlings (Masuma et al., 2011). There are numerous issues associated with the use of wild-caught juveniles for aquaculture, including the unstable supply and the negative impacts on wild stock management (Masuma et al., 2011). As fish are endangered because of wild stock overfishing, the fishing of this species has been controlled based on an assessment by the Western and Central Pacific Fisheries Commission (WCPFC).

To sustain bluefin tuna aquaculture and preserve the wild stocks, research into closed-cycle PBT aquaculture began in the 1970s. In 2002, Kindai University succeeded in closing the full life cycle of PBT (Sawada et al., 2005). Currently, several research institutes and companies in Japan have achieved closed-cycle production of this species (Sawada et al., 2005; Masuma et al., 2011), and have made hatchery-produced tuna seed available for practical tuna aquaculture (Murashita et al., 2021; Okada et al., 2021). Nevertheless, most bluefin tuna aquaculture practices continue to rely on wild-caught juveniles for seed stocks owing to the low productivity of closed-cycle aquaculture (Higuchi et al., 2018; Ienaga et al., 2022). For the conservation of this species and sustainable development of the tuna farming industry, closed-cycle aquaculture should be promoted (Sawada et al., 2013); however, this requires development of technology to improve its productivity.

Sex manipulation in fish to produce mono-sex stocks is an important area in aquaculture research (Budd et al., 2015). Sex manipulation is a prominent tool for achieving several broad goals in aquaculture, including preventing precocious maturation and uncontrolled reproduction, taking advantage of differences in growth rate and economic value of the sexes, reducing the impact of phenotypic sex on product quality, increasing stability of egg production, and protecting the intellectual property of genetically improved strains (Budd et al., 2015). Previous studies have reported that in wild stocks of tuna species, including the Atlantic bluefin

tuna (*T. thynnus*) (Hurley and Iles, 1983), southern bluefin tuna (*T. maccoyii*) (Gunn et al., 2008), bigeye tuna (*T. obesus*) (Farley et al., 2006), albacore (*T. alalunga*) (Chen et al., 2012), and PBT (Shimose et al., 2009), males tend to be larger than females. These findings suggest that in tuna species, males exhibit higher growth performance than females in aquaculture settings. If male-cultured PBT exhibit higher growth performance than females, the production of mono-sex male stocks appears to act as a prominent tool to significantly improve the productivity of closed-cycle PBT aquaculture by shortening production times and reducing production costs.

Sex steroid hormones, specifically estrogens and androgens, play a critical role in fish sex differentiation (Nagahama et al., 2021). Furthermore, environmental, genetic, and social factors strongly influence sex differentiation in fish (Nagahama et al., 2021). Sex manipulation in fish can be achieved using several methods, such as sex steroid hormone administration and temperature treatment (Budd et al., 2015). Sex manipulation techniques are generally developed based on the knowledge of sex differentiation in target fish (Budd et al., 2015), because fish exhibit divergent sex differentiation mechanisms (Nagahama et al., 2021). Despite their ecological and commercial importance, there is almost no data available on sex differentiation mechanisms in tuna species, including PBT. Therefore, to develop appropriate intervention and control strategies for sex in cultured PBT, sex differentiation mechanisms in this fish need to be

characterized in detail.

In chapter 2 of this study, we examined the timing and process of gonadal sex differentiation in PBT using histological and immunochemical analyses. In chapter 3, we revealed the molecular basis of controlling sex differentiation in PBT using comparative and temporal gene expression analyses. In chapter 4, we investigated sexual dimorphism in the growth performance of aquaculture-produced PBT and developed techniques for its sex manipulation based on knowledge accumulated from analyses carried out in chapter 2 and 3. We expect that our study will provide a basis for establishing mono-sex PBT aquaculture, which will contribute to further development of the tuna aquaculture industry and meet conservation objectives for wild PBT stocks.

Chapter 2.

Gonadal sex differentiation and early ovarian/testicular development in cultured Pacific bluefin tuna, *Thunnus orientalis*

Introduction

Detailed and reliable data on gonadal development in aquaculture fish are important for the development of reproductive biotechnologies. For example, knowledge of sex differentiation is vital for the development of sex manipulation technologies. Sexual dimorphism in growth performance is common in fishes, with some species exhibiting superior female growth and others exhibiting superior male growth (Budd et al., 2015; Mei and Gui, 2015). Sex manipulation of stocks is effective in improving aquaculture productivity by shortening production times and reducing production costs (Budd et al., 2015). The ability to control the sex of stocks is also important for achieving several goals in aquaculture, such as the strategic control of reproduction and utilization of differences in economic traits between sexes (Budd et al., 2015). In contrast, studies revealing the mechanisms underlying germ cell development are needed to develop sterilization technologies. Sexual maturation in fish is often accompanied by a reduction in somatic growth and flesh quality (i.e., flesh color, taste, texture, and fat content) as fish divert their energy toward gonadal development (Felip et al., 2001; Piferrer et al., 2009). Sterile fish are a prominent tool for avoiding problems associated with sexual maturation in aquaculture.

Pacific bluefin tuna (*Thunnus orientalis*; hereafter, PBT) is one of the most important species for aquaculture worldwide, particularly in Japan (Masuma et al., 2011). Although

various studies have reported gonadal development in bluefin tunas during adult life stages (Sarasquete et al., 2002; Seoka et al., 2007; Masuma et al., 2011), information regarding this process of gonads at early life stages is scarce. Recently, as a first step toward elucidating the whole process of gonadal development in PBT, we identified the specification and migration patterns of primordial germ cells (PGCs), and the formation process of the gonadal primordium during early embryogenesis and larva development (Higuchi et al., 2019). Here, as a next step, we aimed to reveal the process of differentiation from the gonadal primordium into ovary or testis, and of early ovarian and testicular development during the immature stages in PBT. We expect that our study will provide the necessary basis for future studies on the development of reproductive biotechnologies for PBT.

Materials and Methods

Ethics

All the experiments were performed in accordance with the Guidelines for the Care and Use of Live Fish of the Fisheries Technology Institute (FTI), Japan Fisheries Research and Education Agency (FRA).

Experimental fish and sampling procedure

All sampled PBT were reared from fertilized eggs at the Amami Field Station, FTI, FRA (Kagoshima, Japan). To investigate the process of gonadal sex differentiation, we sampled PBTs at 41, 57, and 83 days post-hatching (dph) between August and September 2019. Furthermore, to investigate the process of early ovarian and testicular development after sex differentiation, we sampled PBTs at 185, 247, 285, 446, and 535 dph from December 2018 to December 2019. All the individual fish were exposed to cold anesthesia. The total length and body weight of each fish sampled were measured. The dissected gonads were fixed with Bouin's solution, stored in 70% ethanol at 4 °C, and then processed for histological analysis and whole-mount immunohistochemistry. The fin or muscle samples of each fish were stored in 300 µl TNES-urea buffer (6 M urea; 10 mM Tris-HCl; pH 7.5; 125 mM NaCl; 10 mM EDTA; 1% SDS) at room temperature according to Asahida et al. (1996), and processed for PCR-based

genetic sex identification.

Histology

The fixed gonads were dehydrated and embedded using standard paraffin-embedding methods. The gonads were then cut into 5 μm-thick sections using a microtome (HistoCore BIOCUT, Leica Biosystems, Wetzlar, Germany) and stained with hematoxylin and eosin (HE). Images of the sections were obtained using a light microscope (BX-43, Olympus, Tokyo, Japan) and a digital camera (DP-70, Olympus). The cross-section area of the gonadal blood vessels was measured from digital images using the image analysis software ImageJ (National Institutes of Health, Bethesda, MD).

Identifying the genetic sex of PBT

Genomic DNA was extracted from PBT fin or muscle samples using the standard phenol-chloroform protocol described by Asahida et al. (1996). After DNA extraction, the genetic sex of each fish was identified using a PCR-based sex identification method based on a male-specific DNA marker, as described by Suda et al. (2019). Briefly, genomic regions, including male-specific segregation, were amplified using male-specific primer sets (forward, 5′ TGCACCTGTAACTCACTAACCG 3′; reverse, 5′ CCTTTTCCTGGCCTCTTTACAT 3′;

product size: 113 base pairs (bp)). An additional primer set for amplifying a segment of beta-*actin* (forward, 5′ GTCCCTGTATGCCTCTGGTC 3′; reverse, 5′ GCAGCTCGTAGCTCTTCTCC 3′; product size: 311 bp) was designed using CLC Main Workbench 8.0.1 (QIAGEN GmbH, Hilden, Germany) as an internal positive control. The following PCR conditions were used: 35 cycles of 30 s denaturation at 94 °C, 30 s annealing at 62 °C for male-specific primers and at 60 °C for beta-*actin* primers, and 30 s extension at 72 °C. Reaction volumes (10 μl) contained 10 ng of DNA template, 0.25 U of *Takara EX Taq* DNA polymerase (Takara Bio, Shiga, Japan), 1 μl of 10X *EX Taq* buffer (Takara Bio), 0.2 mM of dNTPs, and 1 μM of the forward and reverse primers. The PCR products were observed using electrophoresis.

Whole-mount immunohistochemistry

The fixed gonads of PBT sampled at 41 and 57 dph were hydrated and washed with phosphate buffered saline with Tween (PBS-T, 0.01% Tween 20). The gonads were incubated with 10% goat serum (Nichirei Biosciences, Tokyo, Japan) for 1 h at room temperature, and subsequently with primary antibodies against Vasa at 4 °C overnight. A rabbit anti-Vasa antibody (Genetex, Irvine, CA) was used at a 1:100 dilution with Can Get Signal solution A (TOYOBO, Osaka, Japan). The following day, the gonads were washed with PBS-T and

incubated with 2% blocking reagent (Roche, Mannheim, Germany) for 30 min at room temperature. Subsequently, gonads were incubated with secondary antibodies for 1 h at room temperature. The secondary antibody (goat anti-rabbit Alexa Fluor 488, Thermo Fisher Scientific, Waltham, MA) was used at a 1:200 dilution with 2% blocking reagent (Roche). After washing with PBS, the number of germ cells in the gonads was counted under a light microscope (MVX-10, Olympus).

Statistical analysis

Data are presented as the mean ± standard error of the mean (SEM), with the exception of germ cell numbers, which are presented as median values. We tested for differences in the number of germ cells and cross-section area of gonadal blood vessels between sexes during gonadal sex differentiation using Student's *t*-test ($P < 0.05$). Statistical analysis was performed using Prism 7.0 (GraphPad Software, San Diego, CA).

Results

Gonadal sex differentiation in PBT

We histologically characterized the gonads of PBT sampled 41, 57, and 83 dph to investigate the morphological changes in the gonads during sex differentiation (Table 1 and Fig. 1).

At 41 dph, in both presumptive sexes (n = 7 female and 7 male), the gonads were observed as paired cell mass hanging down from the dorsal coelomic wall by short mesenteries in the posterior coelom (Fig. 1A and B). The PGCs surrounded by somatic cells were distributed solitarily and evenly throughout the whole length of the gonads in both sexes (Fig. 1A' and B').

At 57 dph, the first signs of morphological differentiation of the gonads were observed (Fig. 1C and D). In females (n = 7), two elongating somatic cell sheets extended from the dorsal region of the gonad leading to the formation of the ovarian cavity were observed (Fig. 1C). In males (n = 6), a slit-like structure indicating the formation of an efferent duct appeared as a split in the stromal tissue packing the centro-lateral region (Fig. 1D). The number of somatic cells of both sex gonads increased, and blood vessels containing blood cells began to appear in the dorsal region of the gonads (Fig. 1C and D). The cross-section area of the blood vessels in gonads was significantly larger in females (2126.50 ± 294.81 μm^2, n = 5) than in males (687.61 ± 144.90 μm^2, n = 5) ($P < 0.05$) (Fig. 1C and D). The oogonia were solitarily

distributed within the somatic tissue facing the side at which the ovarian cavity was forming (Fig. 1C'), while the type-A spermatogonia were solitarily distributed in the outer region of the gonads (Fig. 1D').

At 83 dph, females had ovaries, as confirmed by the presence of an ovarian cavity with ovarian lamellae (Fig. 1E). The cavities were formed through the fusing of the two elongating somatic cell sheets at their free edge, forming the ovarian cavity of defined ovaries. Meanwhile, in males, efferent ducts, which appeared as slits in the stromal tissue, were observed, and the transverse-section of the gonads had a triangular shape (Fig. 1F). In both sexes, there were more stromal cells, and blood vessels were more expanded than those in the preceding period (Fig. 1E and F). The cross-section area of the blood vessels in gonads was significantly larger in the ovaries (2901.61 ± 620.27 μm^2, $n = 6$) than in the testes (961.72 ± 244.31 μm^2, $n = 4$) ($P < 0.05$) (Fig. 1E and F). The oogonia were solitarily distributed on the sides facing the ovarian cavity (Fig. 1E'), while the type-A spermatogonia were solitarily distributed in the outer region of the testis (Fig. 1F'). At this stage, roundish regions, stained paler by hematoxylin than the outer somatic cell region, appeared in the vicinity of germ cells in gonads of both females and males (Fig. 1E' and F'). At 83 dph, all the PBT gonads sampled were subjected to histological analysis, and the phenotypic sex of all individuals completely matched their genotypic sex (identified using a male-specific DNA marker).

To determine whether proliferation of germ cells affected gonadal sex differentiation in PBT, changes in the number of germ cells during sex differentiation (41 and 57 dph) were investigated using whole-mount immunohistochemistry (Fig. 2). No significant difference in germ cell number was observed between the sexes at the same age (n = 4 fish, $P > 0.05$, Fig. 2C).

Table 1. Details of Pacific bluefin tuna included in this study.

Age (dph)[a]	Number of fish[b]		Total length[c] (cm)	Body weight[c] (g)
	♂	♀		
41	41	27	5.9 ± 0.1	2.1 ± 0.1
57	49	30	11.3 ± 0.1	20.0 ± 0.6
83	4	7	24.1 ± 0.6	187.3 ± 14.8
185	5	5	48.2 ± 0.8	2176.0 ± 117.0
247	1	5	55.1 ± 1.2	3223.3 ± 215.0
285	7	8	59.8 ± 0.9	3794.0 ± 194.1
446	1	4	72.1 ± 0.7	6804.0 ± 267.4
535	1	4	78.9 ± 0.8	9184.0 ± 235.7

[a]dph: days post hatching. [b]The genotypic sex of individuals was identified using a male-specific DNA marker. [c]Total length and body weight are expressed as mean ± standard error of the mean (SEM).

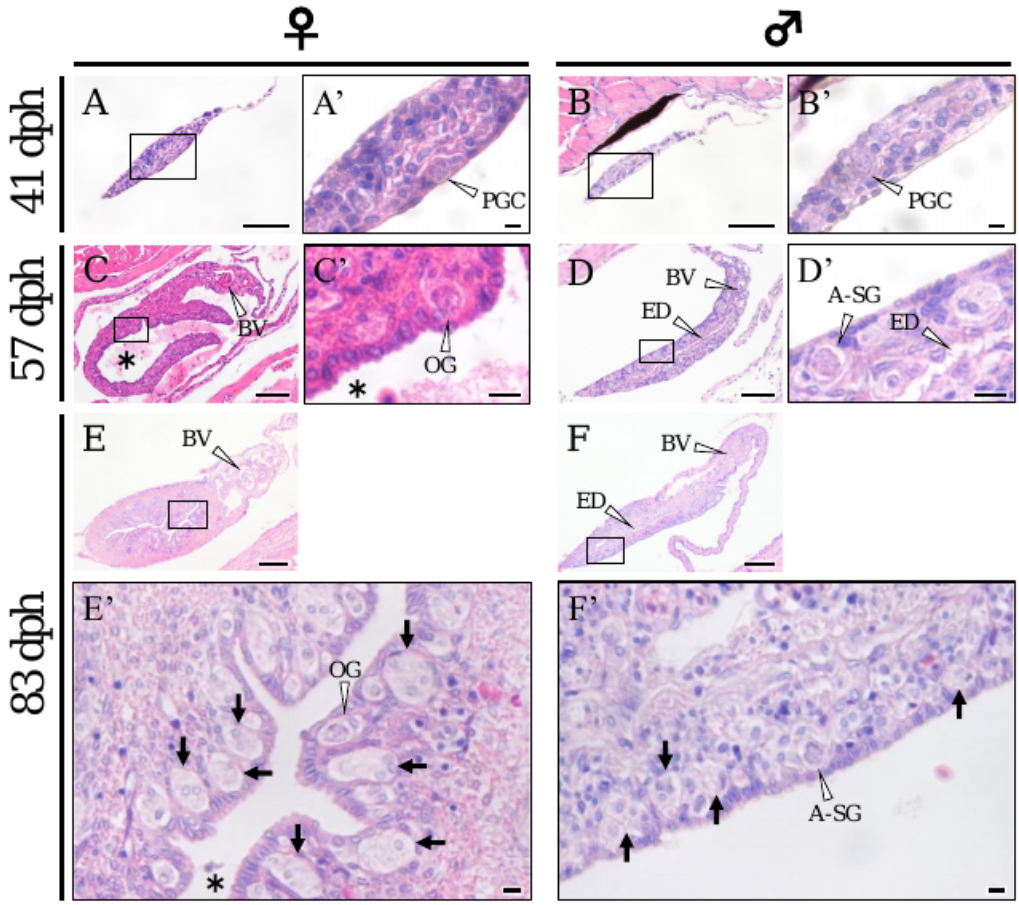

Figure 1. Gonadal sex differentiation in Pacific bluefin tuna sampled 41 (A and B), 57 (C and D), and 83 days post hatching (dph) (E and F). Transverse-sections of gonads were stained with hematoxylin and eosin. The genotypic sex of each fish was identified using male-specific DNA markers. (A and B) At 41 dph, undifferentiated gonads were observed in both sexes. At 57 dph, the formation of the ovarian cavity and the efferent duct was observed in the female and male gonads, respectively. (E and F) At 83 dph, ovaries (confirmed by the presence of an ovarian cavity with ovarian lamellae) and testes (confirmed by the presence of an efferent duct as slits in the stromal tissue with triangular shapes) were observed in female and male PBT, respectively. The insets reveal a higher magnification of the area where the germ cells were located.

Arrowheads indicate the following: PGC, primordial germ cell; OG, oogonia; A-SG, type-A spermatogonia; BV, blood vessels; ED, efferent duct. Arrows indicate roundish regions that appeared during gonadal sex differentiation. Asterisks indicate the ovarian cavity. Scale bars = 50 μm (A–D), 100 μm (E and F), and 10 μm (A'–F').

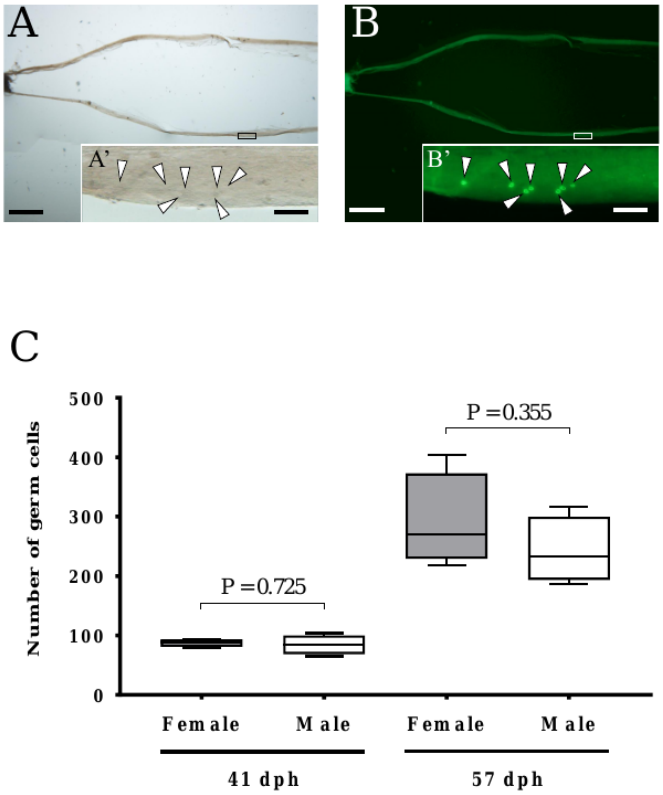

Figure 2. Counting of germ cell number during gonadal sex differentiation in Pacific bluefin tuna by whole-mount immunostaining. (A and B) Brightfield and fluorescent images (left and right columns, respectively) of the gonads of genotypic male PBT at 41 days post hatching (dph) immuno-stained with anti-VASA antibody. The insets reveal a higher magnification of the area where the germ cells were located. Immuno-positive germ cells, indicated by arrowheads, were seen in the gonad. Scale bars = 1 mm (A and B) and 100 μm (A' and B'). (C) The number of germ cells in the gonads of both sexes at 41 and 57 dph. There were no significant differences in germ cell numbers between the sexes at the same age ($P > 0.05$, Student's *t*-test). Boxplots show the 25–75th percentiles (*box*) and the median (*line*) ($n = 4$ fish). *Whiskers* represent maximum and minimum values.

Early ovarian and testicular development in PBT

We histologically characterized the gonads of PBT sampled 185, 247, 285, 446, and 535 dph to investigate the process of early ovarian and testicular development after sex differentiation (Table 1, Fig. 3 and 4).

In females, at 185 dph, oogonia cysts were observed on the sides facing the ovarian cavity (Fig. 3A). At 247 dph, chromatin-nucleolus-stage oocytes, which were larger than oogonia, with cytoplasm showing intense staining by hematoxylin, were observed within the cysts of oogonia (Fig. 3B). At 285 dph, peri-nucleolus-stage oocytes, which were round or oval in shape, with the cytoplasm showing intense staining by hematoxylin and nuclei containing many lightly stained nucleoli, were observed (Fig. 3C). Until 535 dph, the number of peri-nucleolus-stage oocytes increased gradually, although vitellogenic-stage oocytes were not observed (Fig. 3D and E).

In males, at 185 dph, type-A spermatogonia were solitary distributed in the outer region of the testes (Fig. 4A). At 247 and 285 dph, the cysts of type-A spermatogonia were observed (Fig. 4B and C). From 446 dph onwards, the type-A spermatogonia differentiated into type-B spermatogonia, spermatocytes, spermatids, and spermatozoa, although sperms filling the efferent duct were not observed until 535 dph (Fig. 4D–I).

All the PBT gonads sampled from 185 to 535 dph were subjected to histological

analysis, and the phenotypic sex of all individuals completely matched their genotypic sex.

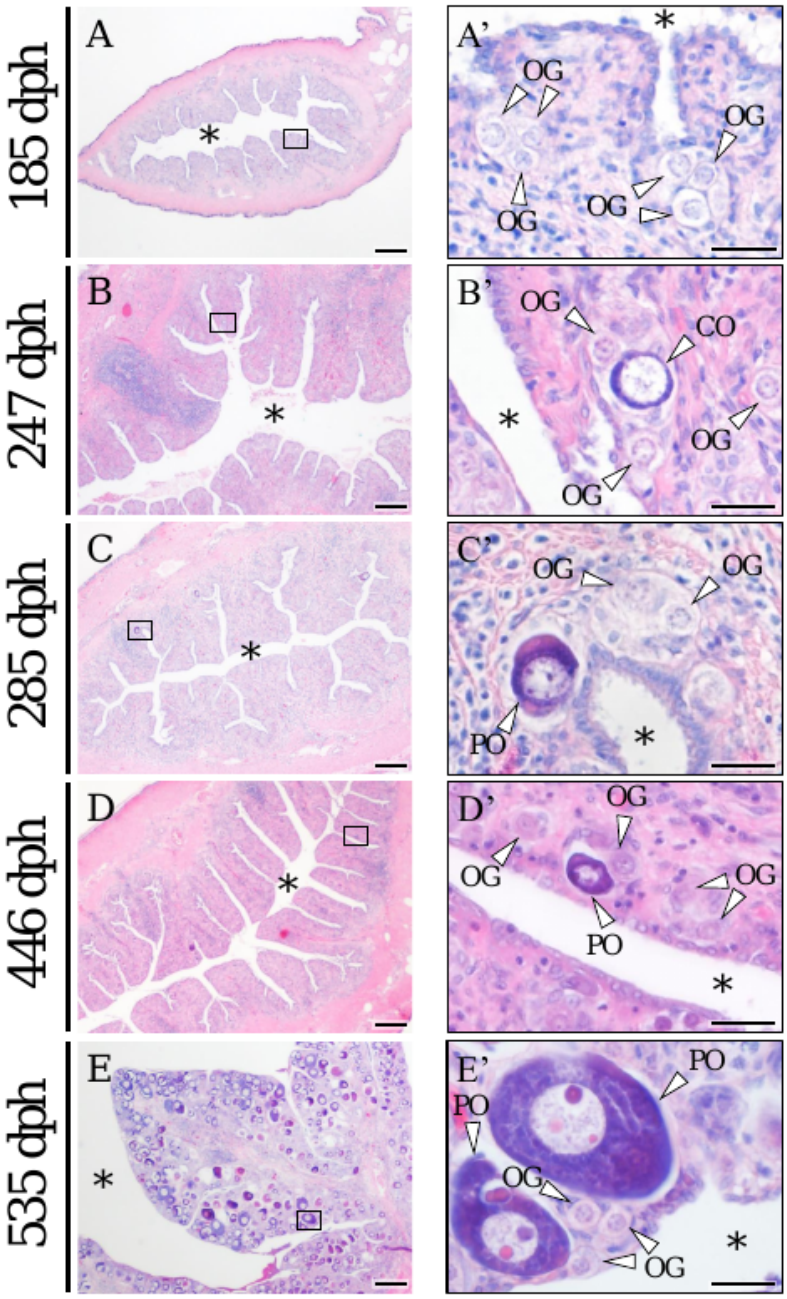

Figure 3. Early ovarian development in Pacific bluefin tuna sampled at 185 (A), 247 (B), 285 (C), 446 (D), and 535 (E) days post hatching (dph). Transverse-sections of ovaries were stained with hematoxylin and eosin. (A) At 185 dph, the cysts of oogonia were observed. (B) During 185–247 dph, oogonia differentiated into chromatin-nucleolus stage oocytes. (C–E) Thereafter,

peri-nucleolus-stage oocytes appeared at 285 dph, and gradually increased in number until 535 dph. The insets reveal a higher magnification of the area where the germ cells were located. Arrowheads indicate the following: OG, oogonia; CO, chromatin-nucleus stage oocytes; PO, peri-nucleolus stage oocytes. Asterisks indicate the ovarian cavity. Scale bars = 100 μm (A–E) and 20 μm (A'–E').

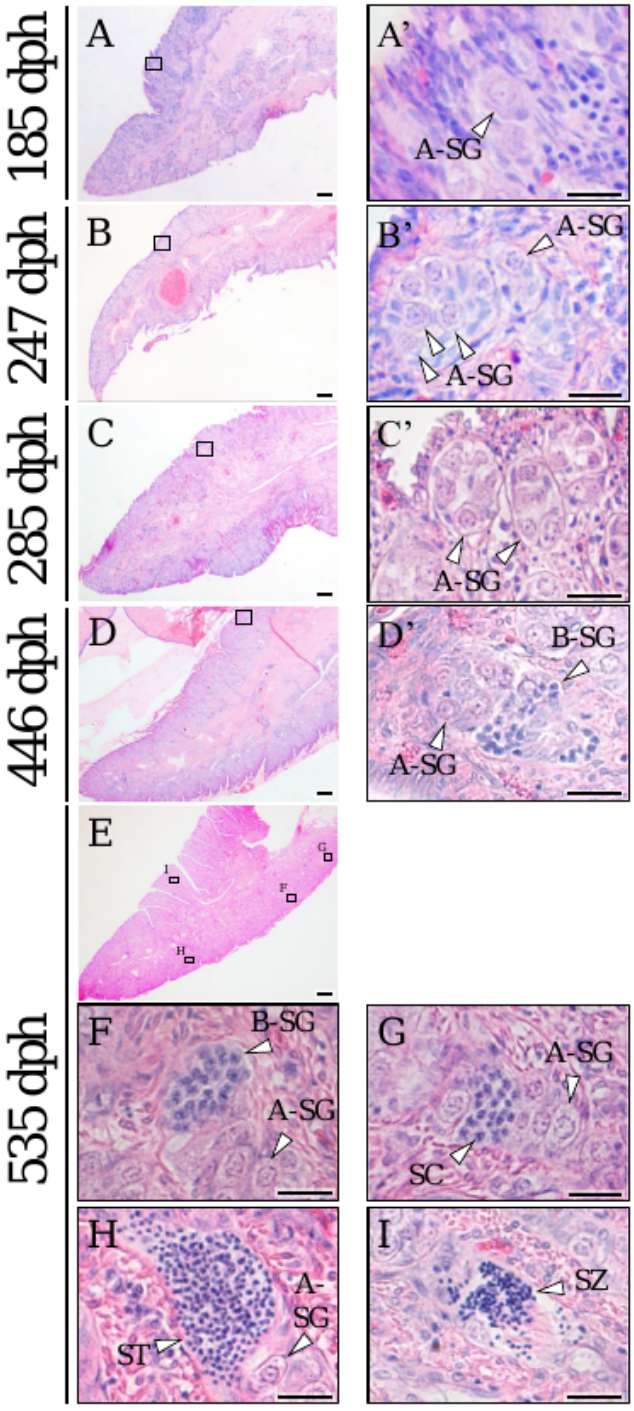

Figure 4. Early testicular development in Pacific bluefin tuna sampled at 185 (A), 247 (B), 285 (C), 446 (D), and 535 (E) days post hatching (dph). Transverse-sections of testes were stained with hematoxylin and eosin. (A) At 185 dph, solitary distributed type-A spermatogonia were

observed. (B and C) At 247 and 285 dph, the cysts of type-A spermatogonia were observed. (D–I) From 446 dph onwards, type-A spermatogonia differentiated into type-B spermatogonia, spermatocyte, spermatid, and spermatozoa. The insets reveal a higher magnification of the area where the germ cells were located. Arrowheads indicate the following: A-SG, type-A spermatogonia; B-SG, type-B spermatogonia; SC; spermatocytes; ST, spermatids; SZ, spermatozoa. Scale bars = 100 μm (A–D), 200 μm (E), and 20 μm (A'–D' and F–I).

Discussion

In this chapter, we demonstrated the morphological changes and timing of gonadal sex differentiation in PBT. Gonadal sex differentiation was first characterized by the formation of the ovarian cavity in females and of the efferent duct in males at 57 dph, and the gonads subsequently differentiated into ovaries or testes according to the genotypic sex until 83 dph. During this period, proliferation and differentiation of germ cells did not differ between sexes: PGCs, oogonia, and type-A spermatogonia were solitarily distributed in gonads. We also showed the developmental process of the ovary and testis during the immature stages of PBT. After gonadal sex differentiation, the gonads of PBTs developed in a sexually dimorphic manner: proliferation and differentiation of germ cells occurred earlier in the ovaries than in the testes. While the oogonia in ovaries formed cysts at 185 dph, the type-A spermatogonia were solitarily distributed in testes at this stage, and cysts of type-A spermatogonia were first observed at 247 dph. Moreover, the oogonia entered meiosis and differentiated into chromatin-nucleolus-stage oocytes until 247 dph, and then into peri-nucleolus-stage oocytes until 285 dph, whereas the type-A spermatogonia differentiated into type-B spermatogonia, spermatocytes, spermatids, and spermatozoa from 446 dph onwards. In contrast, vitellogenic-stage oocytes and sperms filling the efferent duct were not observed in the ovaries and testes, respectively, until 535 dph. Overall, our results provide a basis for future studies on the development of

reproductive biotechnologies, particularly sex manipulation and sterilization technologies, for PBT.

In fish, sex differentiation patterns can be categorized as synchronous hermaphroditism (protandrous and protogynous), gonochorism (undifferentiated and differentiated), or unisexual reproduction (Nakamura et al., 1998; Wootton and Smith, 2014). In this chapter, we demonstrated that the sex differentiation pattern of PBT is a differentiated gonochoristic, because gonads were found to develop directly from an undifferentiated gonad into the ovary or testis. In general, sex development consists largely of two processes: sex determination and subsequent sex differentiation (Devlin et al., 2002). In many gonochoristic fish, sex is determined by genetic factors, that is, males and females have different alleles or even different genes that specify their sexual morphology (Devlin et al., 2002; Kobayashi et al., 2013). Previous studies have suggested that PBT has a male heterogametic system (XX: female, XY: male) (Agawa et al., 2015; Uchino et al., 2016; Suda et al., 2019). In fact, in this chapter, the phenotypic sex of all PBT sampled at the gonadal sex differentiated stage (83 dph) and at later stages (185–535 dph) completely matched their genotypic sex, identified using a previously developed male-specific DNA marker (Suda et al., 2019). These results suggest that gonadal sex determination is triggered by sex-determining factors located on the Y chromosome, and sex differentiation subsequently proceeds according to the sex determination

signal in PBT.

Previous studies on many fish species reported that putative ovaries have more germ cells than putative testes before morphological sex differentiation of gonadal somatic tissues (Strüssmann and Nakamura, 2002; Nakamura, 2013). In medaka, *Oryzias latipes*, shortly after the arrival of germ cells in the gonadal primordium, germ cells resume proliferation in a sexually dimorphic manner. While male germ cells continue to exhibit slow intermittent proliferation, female germ cells initiate fast continuous proliferation and increase in number dramatically (Satoh and Egami, 1972; Hamaguchi, 1982). This sexual dimorphism in the proliferation of germ cells is an important component of ovarian differentiation of gonadal somatic tissues in medaka (Saito et al., 2007; Nakamura et al., 2012). In this chapter, however, the number of germ cells did not differ between the sexes at 41 and 57 dph (the gonadal sex differentiation stage). Our results may indicate that germ cell proliferation does not affect gonadal sex differentiation, and that gonadal somatic tissues in genetic females autonomously differentiate into ovarian tissues in PBT.

In this chapter, we found that blood vessels in gonads appeared to be larger in females than in males during sex differentiation in PBT. Although similar results were observed in pejerrey (*Odontesthes bonariensis*) (Strüssmann et al., 1996; Strüssmann and Nakamura, 2002), little is known about the role of the larger blood vessels in ovarian differentiation. In

PBT, at the gonadal sex differentiation stage (57 dph), while proliferation and differentiation of germ cells did not differ between sexes, female gonads began to elongate their somatic tissues, leading to the formation of the ovarian cavity. These results suggest that larger blood vessels in differentiating PBT ovaries may contribute to ovarian somatic cell/tissue outgrowths by distributing oxygen, nutrients, and hormones.

In this chapter, we found that roundish regions, which are clearly distinguishable from the outer somatic cell region, appeared in the vicinity of germ cells in both sex gonads during sex differentiation in PBT. Based on our observations, the roundish regions in PBT gonads were gradually occupied by germ cells after sex differentiation, and germ cells then proliferated and differentiated in those regions. This remarkable feature has also been observed in golden rabbitfish (*Siganus guttatus*) (Komatsu et al., 2006a). It is widely known that male germ cells proliferate and differentiate into sperm in the testicular lobules (Grier, 1981). Furthermore, a lobule-like structure in the ovary, called the germinal cradle, which is present within the germinal epithelium lined by the basement membrane of the adult ovary, was recently discovered in medaka (Nakamura et al., 2010). The early stages of oogenesis, from germline stem cell/oogonia proliferation to the development of diplotene oocytes, occur in the germinal cradles (Nakamura et al., 2010). Our findings suggest that the roundish regions that appear in PBT gonads during sex differentiation may be a primordium of a structure that supports

proliferation and differentiation of germ cells, reported as lobules in the testis or germinal cradles in the ovary. The germ cells in both lobules and germinal cradles are surrounded by somatic cells, which express supporting cell markers, such as *gsdf* and *sox9b* (Nakamura et al., 2008; Nakamura et al., 2010; Nishimura and Tanaka 2014). To understand the role of the roundish regions in PBT gonads, further studies using these molecular markers are needed.

Chapter 3.

Transcriptome characterization of gonadal sex differentiation in Pacific bluefin tuna, *Thunnus orientalis*

Introduction

Gonadal sex differentiation is crucial in vertebrate sexual reproduction. In gonochoristic fishes (many species of fish are gonochoristic (Devlin et al., 2002)), gonadal primordia are formed at the early embryonic stage and subsequently differentiate into ovaries or testes under the control of various genes and factors (Nagahama et al., 2021). Estrogens are critical factors in fish ovarian differentiation (Guiguen et al., 2010; Li et al., 2019; Nagahama et al., 2021). *Cyp19a1a* (cytochrome P450 aromatase, P450-arom; hereafter, aromatase) is expressed mainly in the female gonads at the onset of sex differentiation, and estrogens synthesized by Aromatase directly induce ovarian differentiation (Guiguen et al., 2010; Li et al., 2019; Nagahama et al., 2021). The transcription factor forkhead box protein L2 (Foxl2) is also a major player in active estrogen biosynthesis as it facilitates *aromatase* expression (Guiguen et al., 2010; Li et al., 2019). By contrast, the physiological roles of androgens in testicular differentiation vary among fish species. For instance, androgen production is absent in the male gonads of Nile tilapia (*Oreochromis niloticus*) during testicular differentiation (Nakamura et al., 2003; Ijiri et al., 2008). Moreover, androgens are actively synthesized in the differentiating male gonads of rainbow trout (*Oncorhynchus mykiss*) (Liu et al., 2000; Govoroun et al., 2001). Doublesex and mab-3 related transcription factor 1 (Dmrt1) is highly conserved and orchestrates testicular differentiation in different vertebrates (Nagahama et al., 2021). Dmrt1 facilitates the

expression of genes regulating testicular differentiation, such as *amh* (anti-Müllerian hormone) in zebrafish (*Danio rerio*) (Webster et al., 2017) and *sox9b* (SRY-box transcription factor 9b) in Nile tilapia (Wei et al., 2019). Dmrt1 may also directly block estrogen production as reported in Nile tilapia (Wang et al., 2010). The gonadal soma-derived factor (Gsdf) also induces testicular differentiation in fish (Nagahama et al., 2021). *Gsdf* upregulation in differentiating male gonads has been confirmed for various fish species (Nagahama et al., 2021). The vital role of Gsdf in testicular differentiation has been demonstrated through loss- and/or gain-of-function studies in several fish species, including Nile tilapia (Kaneko et al., 2015) and medaka (*Oryzias latipes*) (Zhang et al., 2016).

Pacific bluefin tuna (*Thunnus orientalis*; hereafter, PBT) is one of the most important species for aquaculture worldwide (Masuma et al., 2011). As described in chapter 2, we recently demonstrated the timing and morphological process of gonadal sex differentiation in PBT (Hayashida et al., 2021). Furthermore, no difference in germ cell proliferation and differentiation between sexes during gonadal sex differentiation was observed (Hayashida et al., 2021). However, the molecular mechanisms underlying gonadal sex differentiation in PBT remain unclear. Furthermore, although we recently identified a sex determining gene in tuna species, namely *sult1st6y* (sulfotransferase family 1, cytosolic sulfotransferase 6y; Nakamura et al., 2021), data on its expression profile during sex differentiation are lacking. A detailed

understanding of the gonadal sex differentiation mechanisms will provide a fundamental basis for developing reproductive biotechnology in aquaculture, specifically sex-manipulation technologies (Budd et al., 2015).

Application of next-generation sequencing (NGS) technology has recently become increasingly common in the field of aquaculture and fisheries. High-throughput RNA sequencing (RNA-Seq) technology is effective in studying the molecular mechanisms underlying the various biological characteristics of non-model and model species and has high reproducibility. The objective of the present study was to elucidate the molecular mechanisms of gonadal sex differentiation in PBT using NGS technologies. Our research group published the first-draft PBT genome in 2013 (Nakamura et al., 2013) and improved its assembly in 2019 (Suda et al., 2019) and again in 2021 (Nakamura et al., 2021). In this chapter, we initially polished the 2021 version of our PBT draft genome assembly (Nakamura et al., 2021) and predicted the protein coding sequences using the refined genome. Using the predicted gene dataset as a reference, we then examined the global gene expression profiles, including those of *sult1st6y*, of gonadal sex differentiation in PBT via comparative transcriptome analysis based on RNA-Seq technology. Furthermore, we examined the temporal expression profiles of the candidate genes controlling gonadal sex differentiation using quantitative real-time reverse transcription PCR (qRT-PCR).

Materials and Methods

Ethics statement

All experiments were conducted in accordance with the Guidelines for the Care and Use of Live Fish of the Fisheries Technology Institute (FTI) of the Japan Fisheries Research and Education Agency (FRA) and the ARRIVE guidelines. All experiments were approved by the Institutional Animal Care and Use Committee of FTI.

Draft genome improvement and protein coding sequence prediction

The draft genome sequence for male PBT consisted of 948 scaffolds and was previously published in 2021 (Nakamura et al., 2021). This sequence was polished with PolishCLR (Rhie et al., 2021) (https://github.com/isugifNF/polishCLR) using the Pacific Biosciences (PacBio) and Illumina data from the previous version. Genome completeness was evaluated and compared against that of the previous version using BUSCO (Manni et al., 2021) v. 5.3.0 (https://gitlab.com/ezlab/busco/-/releases#5.3.0) and the Actinopterygii ortholog set. The protein-coding sequences were predicted with reference to those from the PBT genome published in 2013 (Nakamura et al., 2013), the genome of Southern bluefin tuna (*Thunnus maccoyii*) in the GenBank (Sayers et al., 2020) (https://www.ncbi.nlm.nih.gov/genbank/), and five model fish genomes in the Ensembl database (Howe et al., 2021) (release 104)

(https://www.ensembl.org/index.html?redirect=n0), including zebrafish, stickleback (*Gasterosteus aculeatus*), medaka, tiger puffer (*Takifugu rubripes*), and tetraodon (*Tetraodon nigroviridis*). The foregoing protein sequences were mapped to the current PBT genome with Exonerate (Slater and Birney, 2005) v. 2.4.0 (https://anaconda.org/bioconda/exonerate). All prediction results were merged, excluding overlapping loci with lower alignment scores. The predicted protein sequences were compared with those of two model fishes, zebrafish and medaka (Ensembl database, Release 104), using the BLASTP program (E-value < $1.0E^{-4}$).

Sample collection and RNA extraction and sequencing

PBT gonads at the sex-differentiated stage (Fig. 5a) were collected at 100 days post hatching (dph) from fish reared from fertilized eggs. The oogonia and type-A spermatogonia were solitarily distributed in the differentiated ovary and testis. The total length and body weight of all PBTs sampled were 25.6 ± 11.5 cm and 258.4 ± 94.5 g (n = 10 fish, mean ± standard error of the mean (SEM)), respectively. Dissected gonads were stored in RNAlater (Ambion, Austin, TX) at −30 °C until RNA extraction. The sex phenotypes and genotypes of each fish were determined via histological observation and PCR-based genotypic sex identification, respectively (Suda et al., 2019; Hayashida et al., 2021). All fish gonads differentiated into ovaries or testes according to their sex genotypes.

Total RNA was extracted from the gonads, and RNA extracts were treated with DNase using the RNeasy Mini kit (Qiagen GmbH, Hilden, Germany) according to the manufacturer's instructions. The concentration and quality of purified total RNA were determined using NanoDrop One (Thermo Fisher Scientific, Waltham, MA) and the Agilent 2200 TapeStation System with RNA screen tape (Agilent Technologies, Santa Clara, CA). High-quality RNA extracts with RNA integrity number (RIN) > 7 were selected from three fish per sex (Table 2). The cDNA libraries were constructed using 1 μg total RNA and Illumina Stranded mRNA Prep (Illumina, San Diego, CA) according to the manufacturer's instructions. The libraries were sequenced into 75-bp paired end reads using NextSeq 500 systems (Illumina). The raw data were demultiplexed, trimmed of adapters, and converted into the FASTQ format using bcl2fastq v. 2.20 (Illumina).

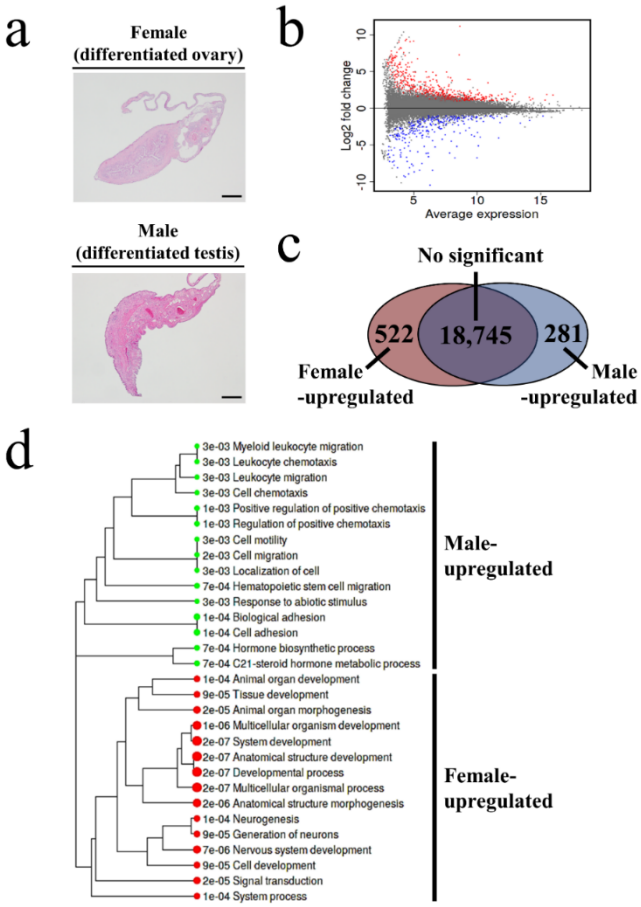

Figure 5. Summary of comparative transcriptome analysis. (a) Histological micrographs of sex-differentiated-stage Pacific bluefin tuna gonads subjected to RNA sequencing. Bars = 200 μm. (b) MA plot showing differentially expressed genes. Significantly upregulated ($P < 0.05$) genes in females and males are indicated by red and blue dots, respectively. Genes not significantly different between sexes ($P > 0.05$) are indicated by gray dots. (c) Venn diagram showing numbers of commonly ($P > 0.05$) and differentially ($P < 0.05$) expressed genes between sexes. (d) Hierarchical clustering tree showing the top 15 enriched Gene Ontology (GO) biological process terms in upregulated genes for each sex. The circle size and number on the left side of each GO term indicate false discovery rate adjusted *P*-values.

Table 2. Results of RNA sequencing.

Sample	RNA Integrity No. (RIN)	No. reads	No. clean reads	No. clean bases (Gb)	GC content (%)	Total No. mapped reads (%)
Female-1	9.2	79,685,638	79,682,070	5.21	47.6	90.7
Female-2	8.9	75,238,374	75,234,984	4.92	47.3	90.7
Female-3	8.3	102,356,556	102,352,454	6.70	47.0	90.3
Male-1	7.3	81,855,526	81,852,002	5.36	46.9	89.9
Male-2	8.2	77,421,316	77,417,522	5.07	46.7	90.6
Male-3	7.7	78,289,102	78,285,284	5.12	46.9	90.1

Comparative transcriptome analysis

RNA-Seq data analysis was performed using the CLC Genomics Workbench v. 12.0.3 (QIAGEN GmbH). Raw reads were trimmed with default parameters (quality limit = 0.05 and ambiguous limit = 2), and the trimmed reads were mapped onto the reference sequences with default parameters (mismatch cost = 2, insertion cost = 3, deletion cost = 3, length fraction = 0.8, and similarity fraction = 0.8). The read count files containing the values of the reads mapped against the reference sequences were then loaded into the integrated Differential Expression and Pathway analysis (iDEP) web platform (Ge et al., 2018) (http://bioinformatics.sdstate.edu/idep/). The data were then normalized using DEseq2 (Love et al., 2014) (https://bioconductor.org/packages/release/bioc/html/DESeq2.html). The DESeq2 program in iDEP was also used to identify differentially expressed genes between sexes. The false discovery rate and minimum fold change cutoff/threshold values were set to 0.05 and 2, respectively. The differentially expressed genes were then subjected to enrichment analysis in the GO biological process database using the Ensembl zebrafish gene IDs (Release 104) in iDEP.

qRT-PCR

Previously sampled PBT gonads (Hayashida et al., 2021) were stored in RNAlater

(Ambion) at −30 °C until RNA extraction. Total RNA was extracted using ISOGEN (Nippon Gene, Toyama, Japan) and then treated with TURBO DNase (Ambion) according to the manufacturer's instructions. A 1 µl aliquot of the total RNA was used for quantification with a NanoDrop spectrometer (ND-1000, Thermo Fisher Scientific). The quantified RNA samples were used for qRT-PCR with a one-step RT-PCR system using the One Step TB Green PrimeScript PLUS RT-PCR Kit (Takara Bio, Shiga, Japan). The reactions were run on a Light Cycler 480 instrument (Roche, Mannheim, Germany) in 96-well plates (Roche). The reaction volumes (20 µl) contained 10 ng of the total RNA template, 10 µl of 2× One Step TB Green RT-PCR Buffer 4, 1.2 µl of TaKaRa Ex *Taq* Hs Mix, 0.4 µl of PrimeScript PLUS RTase Mix, and 0.4 µM each of forward and reverse primers, except for *anxa1b* (annexin A1b), where the amount of each forward and reverse primer was 0.1 µM. The gene-specific primers and PCR amplification conditions are shown in Table 3. The primers were designed using CLC Main Workbench v. 8.0.1 (QIAGEN GmbH). The quantification standard was a plasmid containing the partial cDNA sequence of a target gene. Standard seven-point sets ranged from 1×10^8 to 1×10^2 copies and were prepared using tenfold serial dilutions. Technical duplicates were performed for all experimental samples and standards. The intra-assay coefficient of variation (CV) was determined using repeated standard sample measurements (n = 8) (Table 3). The expression levels are presented as means ± SEM.

Table 3. Primer sequences, PCR conditions, and coefficient of variation (CV) used in quantitative real-time reverse transcription PCR analysis.

Target	Primer (5'-3')	Amplification reaction	Coefficient of variation (CV; %)
cyp19a1a (g2700)	Forward: CTGTTGTAGGTGACAGACAG Reverse: CACGACGCATGGTGAAGTC	45 cycles of 95 °C for 5 s and 60 °C for 20 s	0.25
cyp11c1 (g16537)	Forward: CCACTACTGAAAGGCACAA Reverse: CGGCAGGTATGTGGTAAT	40 cycles of 95 °C for 5 s and 60 °C for 20 s	0.28
hsd11b2 (g28927)	Forward: CCTGCCCTCCTCCTATAA Reverse: TAATCCTCTAGCAGCGCC	40 cycles of 95 °C for 5 s and 60 °C for 20 s	0.30
foxl2 (g17853)	Forward: GTAAATTCCCCTTCTATGAG Reverse: ATTCCCTTTTCTCTCCCC	40 cycles of 95 °C for 5 s and 60 °C for 30 s	0.68
dmrt1 (g7920)	Forward: ATGAGCAAGGACAAGCAG Reverse: CTCTGCCTCTCAGCTATAA	50 cycles of 95 °C for 5 s, 55 °C for 30 s, and 72 °C for 30 s	0.46
gsdf (g4772)	Forward: CGGTGGAAACAGTACAAG Reverse: ATTGGTGTGGGATGATGG	35 cycles of 95 °C for 5 s, 55 °C for 30 s, and 72 °C for 30 s	0.68
sult1st6y (g29404)	Forward: AATCAGGGACAACGTGGATG Reverse: CTCTTGGGGGATCCATTTTC	40 cycles of 95 °C for 5 s, 60 °C for 60 s	0.48
gldn (g2699)	Forward: GAGAAGCCAGTAAAGAAGAA Reverse: CACCACACGACCAGAAAA	40 cycles of 95 °C for 5 s and 60 °C for 30 s	0.93
irx3a (g3224)	Forward: GTGGGGAAAGAGGGTAAAG Reverse: GAAGAGTGGTGATGGTGG	40 cycles of 95 °C for 5 s and 62 °C for 30 s	0.38
vangl1 (g5686)	Forward: TCCTCACCACACTCACAC Reverse: CACAAGGGACACGGCAAA	40 cycles of 95 °C for 5 s and 60 °C for 30 s	0.87
anxa1b (g5180)	Forward: AAACAACGAGCAGAGACA Reverse: TTCATCCAGCTTCTTCCCA	40 cycles of 95 °C for 5 s and 62 °C for 30 s	0.41
cldn11a (g10146)	Forward: AATGTGTGGTATGGTGTC Reverse: AGTAGGGAGAAGATGGTG	40 cycles of 95 °C for 5 s, 60 °C for 30 s, and 72 °C for 30 s	0.50
tnn (g11982)	Forward: TACCTACCAACACGACACC Reverse: ACACACCTCCCATCCACA	40 cycles of 95 °C for 5 s and 62 °C for 30 s	0.19

Statistical analysis

For the comparative transcriptome analysis, statistical analyses were conducted in iDEP. For the temporal gene expression comparison using qRT-PCR, the statistical analyses included Welch's *t*-test (between sexes at each sampling period) and one-way analysis of variance (ANOVA), followed by Tukey's multiple comparisons test (for the expression trends in each sex). Statistical analyses of the qRT-PCR data were performed in GraphPad Prism v. 7.0 (GraphPad Software, San Diego, CA). Statistically significant differences were determined at $P < 0.05$.

Results

Reference gene dataset construction using a polished draft genome

The 2021 version of the PBT draft genome (Nakamura et al., 2021) was rearranged from 948 to 580 scaffolds by polishing the sequence and eliminating redundancy. The completeness score obtained via Benchmarking Universal Single-Copy Orthologs (BUSCO) assessment, i.e., the reference ortholog capture ratio of the older version, was 98.2%, of which 95.7% were singletons and 2.5% were duplicates (Nakamura et al., 2021). This ratio was 98.4% for the current version, of which 97.7% were singletons and 0.7% were duplicates. Few of the doubly predicted orthologs in the previous version (~2% of 3640 reference genes) (Nakamura et al., 2021) were predicted as singletons by removing redundant scaffolds. We predicted 30,156 protein-coding sequences from the current PBT genome (see Supplementary Data 1 online; https://doi.org/10.1038/s41598-023-40914-y). Of these, ~90% resembled those corresponding to the zebrafish and medaka protein sequences (see Supplementary Table S1 online; https://doi.org/10.1038/s41598-023-40914-y).

RNA-Seq and comparative transcriptome analyses

Table 2 summarizes the RNA-Seq results. Sequencing of the cDNA libraries yielded 75–102 million paired-end reads (75 bp). Over 99% of the sequenced reads were clean

following quality control. Clean reads (89.9–90.7%) were read-mapped to the reference sequences.

The PBT gonads at the sex-differentiated stage (Fig. 5a) were subjected to comparative transcriptome analysis (Fig. 5b and 5c). A total of 522 and 281 genes were significantly upregulated in the females and males, respectively ($P < 0.05$, see Supplementary Table S2 online; https://doi.org/10.1038/s41598-023-40914-y). Both sexes shared the expression of 18,745 genes ($P > 0.05$, see Supplementary Table S3 online; https://doi.org/10.1038/s41598-023-40914-y). Fig. 5d and Supplementary Tables S4–S5 (see online; https://doi.org/10.1038/s41598-023-40914-y) show the top 15 Gene Ontology (GO) biological process terms enriched in each sex from the genes differentially expressed between sexes. In the females, several cell/tissue development-related terms, including ‘animal organ development’ (GO:0048513), ‘tissue development’ (GO:0009888), ‘animal organ morphogenesis’ (GO:0009887), ‘multicellular organism development’ (GO:0007275), ‘system development’ (GO:0048731), ‘anatomical structure development’ (GO:0048856), ‘developmental process’ (GO:0032502), ‘multicellular organismal process’ (GO:0032501), ‘anatomical structure morphogenesis’ (GO:0009653), ‘cell development’ (GO:0048468), and ‘system development’ (GO:0003008) were detected. In the males, structural development-related terms, such as ‘cell motility’ (GO:0048870), ‘cell migration’ (GO:0016477),

‘localization of cell’ (GO:0051674), ‘biological adhesion’ (GO:0022610), and ‘cell adhesion’ (GO:0007155) were detected. The steroidogenesis-related terms ‘hormone biosynthetic process’ (GO:0042446) and ‘C21-steroid hormone metabolic process’ (GO:0008207) were also detected in the males.

The expression profiles of the genes enriched in several GO terms was exemplary validated using qRT-PCR (Fig. 6). The qRT-PCR targeted three upregulated genes for each sex: *gldn* (gliomedin; contig No. g2699), *irx3a* (iroquois homeobox 3a; contig No. g3224), and *vangl1* (VANGL planar cell polarity protein 1; contig No. g5686) in female, and *anxa1b* (contig No. g5180), *cldn11a* (claudin 11a; contig No. g10146), and *tnn* (tenascin N; contig No. g11982) in males (Table S4–S5). Furthermore, their temporal expression during gonadal sex differentiation was identified. In the females, *gldn*, *irx3a*, and *vangl1* expression significantly increased from the morphologically sex-undifferentiated (41 dph) to the differentiated (83 dph) stages ($P < 0.05$). However, in males, *gldn*, *irx3a*, and *vangl1* expression remained low until the differentiated stage. The *gldn*, *irx3a*, and *vangl1* expression levels were significantly higher in females than in the males at the differentiating (57 dph) and differentiated (83 dph) stages ($P < 0.05$). In males, *anxa1b* and *cldn11a* expression significantly increased from the undifferentiated (41 dph) to the differentiated (83 dph) stages ($P < 0.05$), and *cldn11a* and *tnn* expression significantly increased from the undifferentiated (41 dph) to the differentiating (57 dph) stages

($P < 0.05$). In females, *anxa1b*, *cldn11a*, and *tnn* expression remained low until the differentiated stage. The *anxa1b*, *cldn11a*, and *tnn* expression levels were significantly higher in males than in females at the differentiated stage (83 dph; $P < 0.05$). The *cldn11a* and *tnn* expression levels were also significantly higher in males than in females at the differentiating stage (57 dph; $P < 0.05$). *Cldn11a* expression was also significantly higher in males than in females at the undifferentiated stage (41 dph; $P < 0.05$).

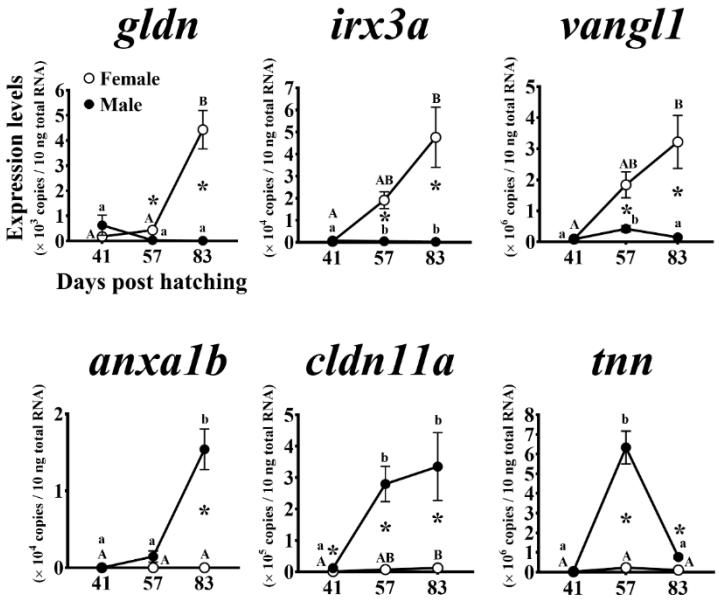

Figure 6. Temporal expression patterns of genes encoding unreported factors in fish sex differentiation during gonadal sex differentiation in Pacific bluefin tuna. Quantitative real-time reverse transcription (qRT-PCR) targeted three genes for each sex, which were enriched in multiple Gene Ontology (GO) pathways (*gldn*, *irx3a*, and *vangl1* in females, and *anxa1b*, *cldn11a*, and *tnn* in males; see Supplementary Table S4–S5 online; https://doi.org/10.1038/s41598-023-40914-y). Total RNA extracted from the gonads of each sex at morphologically sex-undifferentiated (41 days post-hatching (dph)), differentiating (57 dph), and differentiated (83 dph) stages (Hayashida et al., 2021) were subjected to qRT-PCR. Open and closed circles indicate genotypic females and males, respectively. Bars indicate the mean ± standard error of the mean (SEM) (n = 3 fish). Different letters indicate significant differences ($P < 0.05$, one-way ANOVA followed by Tukey's multiple comparisons test). Asterisks indicate significant differences between sexes at each age ($P < 0.05$, Welch's t-test).

Sex steroid synthesis-related gene expression patterns

A comparative transcriptome analysis disclosed sexual dimorphism in sex steroid synthesis-related gene expression (Fig. 7a). *Star* (steroidogenic acute regulatory protein, StAR; contig No. g8869), *cyp11a2* (cytochrome P450 cholesterol side-chain cleavage enzyme, P450-scc; contig No. g1984), *cyp17a1* (cytochrome P450 17α-hydroxylase/C17-C20 lyase, P450-c17; contig No. g4434), *cyp17a2* (P450-c17; contig No. g26576), *cyp11c1* (cytochrome P450 family 11 subfamily C polypeptide 1, P450-c11; contig No. g16537), and *hsd11b2* (11β-hydroxysteroid dehydrogenase, 11β-HSD; contig No. g28927) were significantly upregulated in males ($P < 0.05$). *Aromatase* (contig No. g2700) was significantly upregulated in females ($P < 0.05$). There were no significant differences between sexes in terms of their *hsd3b7* (3β-hydroxysteroid dehydrogenase, 3β-HSD; contig No. g17096) and *hsd17bs* (17β-hydroxysteroid dehydrogenase, 17β-HSDs; see Supplementary Fig. S1 online; https://doi.org/10.1038/s41598-023-40914-y) expression levels ($P > 0.05$). *Hsd20b2* (20β-hydroxysteroid dehydrogenase, 20β-HSD; contig No. g14056) was not expressed in either sex.

The qRT-PCR identified the temporal expression of the genes encoding estrogen and androgen biosynthesis-related enzymes (*aromatase*, *cyp11c1*, and *hsd11b2*) during gonadal sex differentiation (Fig. 7b). In females, *aromatase* expression significantly increased from the morphologically sex-undifferentiated (41 days post-hatching (dph)) to the differentiating (57

dph) stages ($P < 0.05$) and remained high until the differentiated stage (83 dph). In males, however, *aromatase* expression remained low until the differentiated stage. The *aromatase* expression was significantly higher in females than in males at all stages (41–83 dph; $P < 0.05$). In males, *cyp11c1* expression significantly increased from the differentiating (57 dph) to the differentiated (83 dph) stages ($P < 0.05$). In females, however, it remained low until the differentiated stage. In males, *hsd11b2* expression significantly increased from the undifferentiated (41 dph) to the differentiating (57 dph) stages ($P < 0.05$) and increased further until the differentiated (83 dph) stage ($P < 0.05$). In females, however, it remained low until the differentiated stage. *Cyp11c1* and *hsd11b2* expression levels were significantly higher in males than in females at the differentiating (57 dph) and differentiated (83 dph) stages ($P < 0.05$).

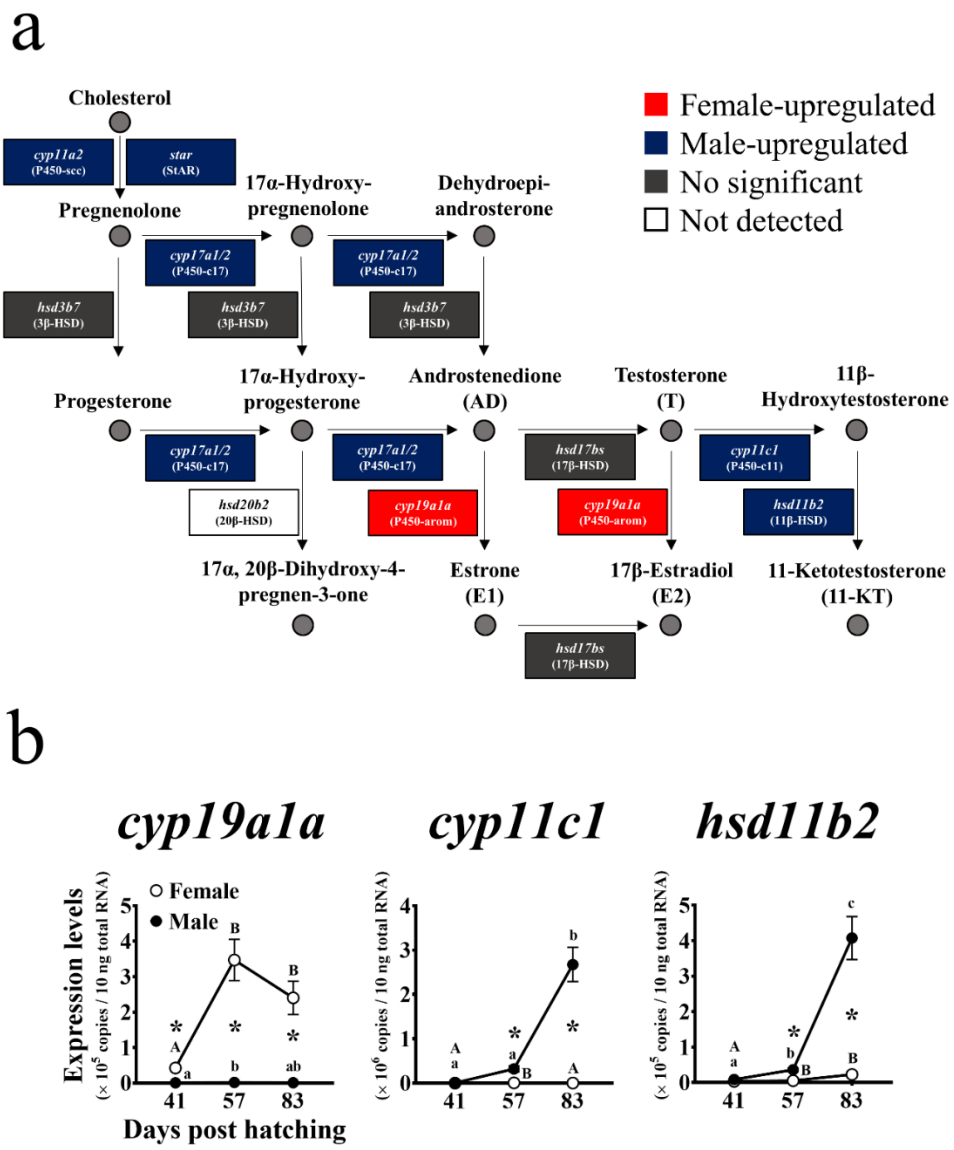

Figure 7. (a) Expression patterns of sex steroid biosynthesis-related genes in gonads of Pacific bluefin tuna at the sex differentiated stage. The diagram shows gonadal sex steroid biosynthesis pathways in fish (Young et al., 2005; Rajakumar and Senthilkumaran, 2020). Upregulated genes in females and males are indicated by red and blue boxes, respectively ($P < 0.05$). Genes not significantly different between sexes are indicated by gray boxes ($P > 0.05$). The gene with no detectable expression is indicated by a white box. Expression patterns of genes encoding 17β-

hydroxysteroid dehydrogenases (17β-HSDs) are shown in Supplementary Fig. S1 (https://doi.org/10.1038/s41598-023-40914-y). (b) Temporal expression patterns of genes encoding key enzymes in estrogen and androgen biosynthesis during gonadal sex differentiation in Pacific bluefin tuna. Total RNA extracted from gonads in each sex at morphologically sex-undifferentiated (41 days post-hatching (dph)), differentiating (57 dph), and differentiated (83 dph) stages (Hayashida et al., 2021) was subjected to quantitative real-time reverse transcription PCR. Open and closed circles indicate genotypic females and males, respectively. Bars indicate mean ± standard error of the mean (SEM) (n = 3 fish). Different letters indicate significant differences ($P < 0.05$, one-way ANOVA followed by Tukey's multiple comparisons test). Asterisks indicate significant differences between sexes at each age ($P < 0.05$, Welch's t-test).

Sex differentiation-related gene expression patterns

A comparative transcriptome analysis revealed sexual dimorphism in sex differentiation-related gene expression (Fig. 8a). *Foxl2* (contig No. g17853) and *aromatase* were significantly upregulated in females ($P < 0.05$), whereas *dmrt1* (contig No. g7920) and *gsdf* (contig No. g4772) were significantly upregulated in males ($P < 0.05$). There were no significant differences between sexes in terms of their *amh* (contig No. g11182), *amhr2* (anti-Müllerian hormone receptor type 2; contig No. g370), *sox9a* (SRY-box transcription factor 9a; contig No. g15913), and *sox9b* (contig No. g14928) expression levels ($P > 0.05$).

The qRT-PCR identified the temporal expression of the sex differentiation-related genes with sexually dimorphic expression during gonadal sex differentiation (Fig. 8b). In females, *foxl2* expression significantly increased from the differentiating (57 dph) to the differentiated (83 dph) stages ($P < 0.05$). In males, however, *foxl2* expression remained low until the differentiated stage. *Foxl2* expression was significantly higher in females than in males at all stages (41–83 dph; $P < 0.05$). In males, *dmrt1* and *gsdf* expression levels significantly increased from the undifferentiated (41 dph) to the differentiating (57 dph) stages ($P < 0.05$) and remained high until the differentiated stage (83 dph). In females, however, *dmrt1* and *gsdf* expression levels remained low until the differentiated stage. *Dmrt1* and *gsdf* expression levels were significantly higher in males than in females at the differentiating (57 dph) and

differentiated (83 dph) stages ($P < 0.05$).

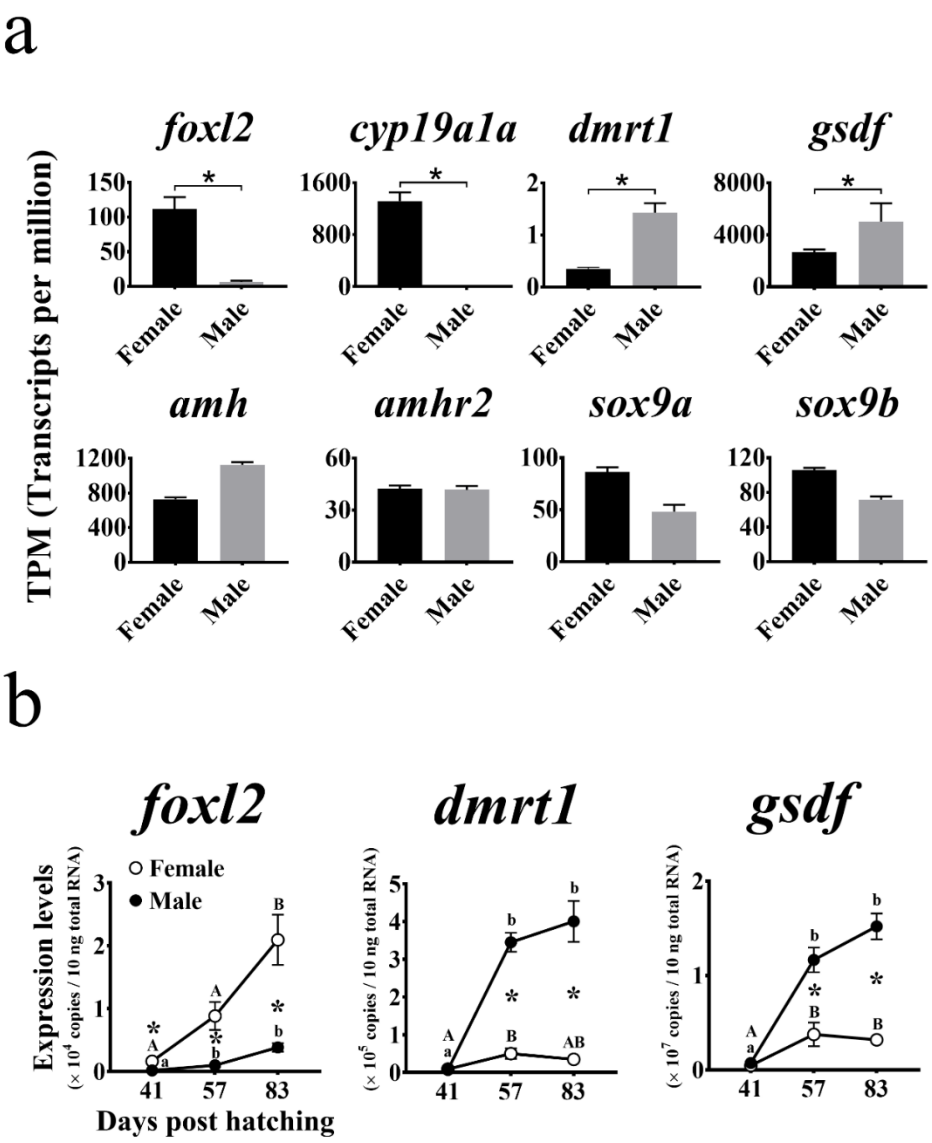

Figure 8. (a) Sex differentiation-related gene expression patterns in Pacific bluefin tuna gonads at the sex-differentiated stage. Expression levels correspond to transcripts per million (TPM). Statistical differences indicated by asterisks are false discovery rate-adjusted *P*-values ($P < 0.05$). (b) Temporal expression patterns of genes identified via comparative transcriptome analysis as candidate gonadal sex differentiation regulators in Pacific bluefin tuna. Total RNA extracted from the gonads of each sex at morphologically sex-undifferentiated (41 days post-

hatching (dph)), differentiating (57 dph), and differentiated (83 dph) stages (Hayashida et al., 2021) was subjected to quantitative real-time reverse transcription PCR. Open and closed circles indicate genotypic females and males, respectively. Bars indicate mean ± standard error of the mean (SEM) (n = 3 fish). Different letters indicate significant differences ($P < 0.05$, one-way ANOVA followed by Tukey's multiple comparisons test). Asterisks indicate significant differences between sexes at each age ($P < 0.05$, Welch's t-test).

Candidate sex-determining gene expression patterns

Comparative transcriptome analysis showed that the candidate sex-determining gene in PBT, *sult1st6y* (contig No. g29404), was significantly upregulated in males ($P < 0.05$; Fig. 9a). qRT-PCR analysis revealed that the expression of *sult1st6y* was specifically increased in males during sex differentiation (Fig.9b). In males, *sult1st6y* expression significantly increased from the morphologically sex-undifferentiated (41 dph) to the differentiating (57 dph) stages ($P < 0.05$) and further significantly increased until the differentiated stage (83 dph; $P < 0.05$). *Sult1st6y* expression was significantly higher in males than in females at all stages (41–83 dph; $P < 0.05$).

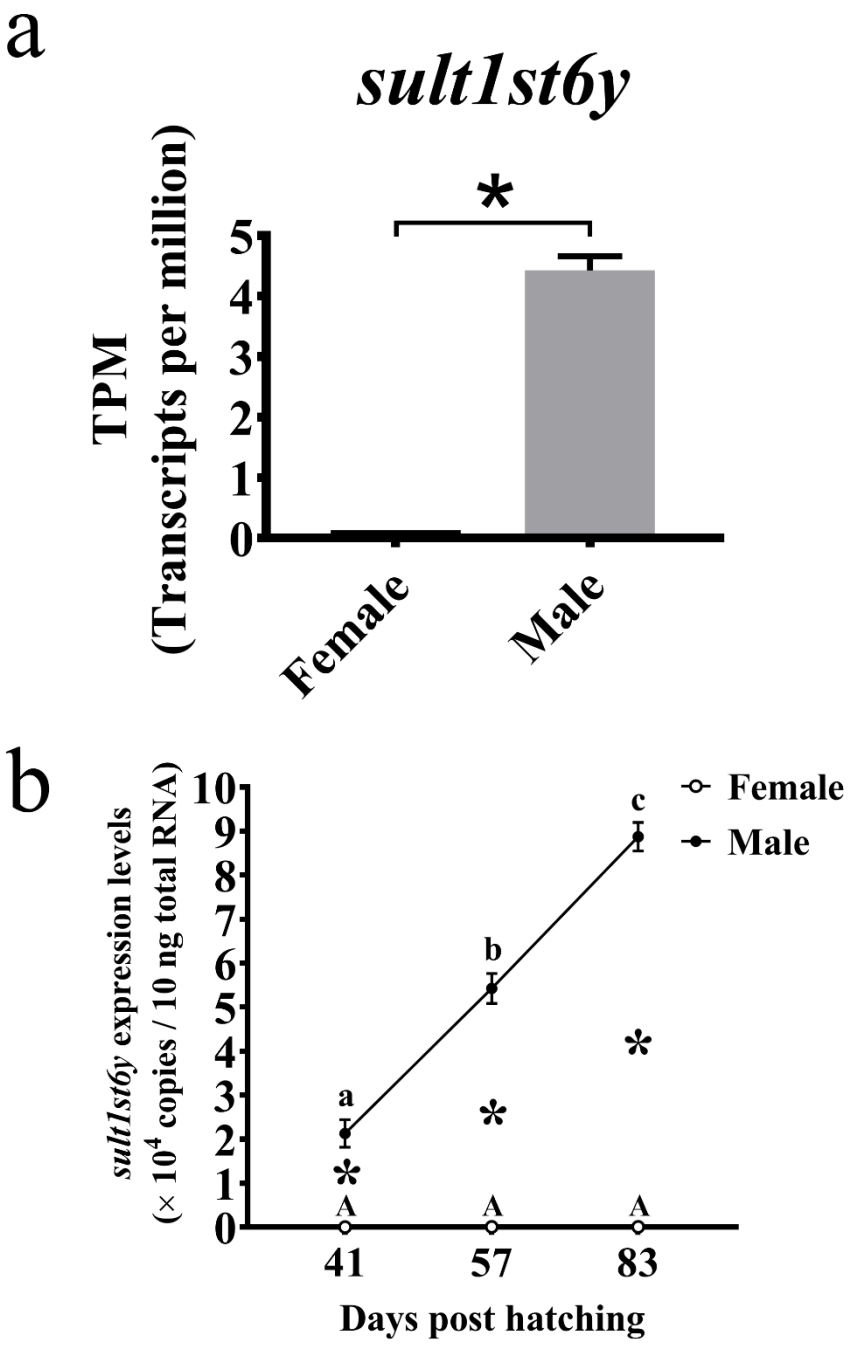

Figure 9. (a) Expression pattern of candidate sex-determining gene, *sult1st6y* (sulfotransferase family 1, cytosolic sulfotransferase 6y; Nakamura et al., 2021), in Pacific bluefin tuna gonads at the sex-differentiated stage. Expression levels correspond to transcripts per million (TPM). Statistical differences indicated by asterisks are false discovery rate-adjusted *P*-values ($P <$

0.05). (b) Temporal expression pattern of *sult1st6y* during sex differentiation in Pacific bluefin tuna. Total RNA extracted from the gonads of each sex at morphologically sex-undifferentiated (41 days post-hatching (dph)), differentiating (57 dph), and differentiated (83 dph) stages (Hayashida et al., 2021) was subjected to quantitative real-time reverse transcription PCR. Open and closed circles indicate genotypic females and males, respectively. Bars indicate mean ± standard error of the mean (SEM) (n = 3 fish). Different letters indicate significant differences ($P < 0.05$, one-way ANOVA followed by Tukey's multiple comparisons test). Asterisks indicate significant differences between sexes at each age ($P < 0.05$, Welch's t-test).

Discussion

In this chapter, we initially updated our draft genome assembly for PBT. The completeness scores indicate that the current polished genome was slightly improved compared to the previous version (Nakamura et al., 2021). Thereafter, we transcriptomically characterized gonadal sex differentiation in PBT using a reference gene dataset predicted from the polished draft genome. A comparative transcriptome analysis based on RNA-Seq identified 19,548 genes expressed in the PBT gonads at the sex-differentiated stage. Of these, 522 and 281 genes were upregulated in females and males, respectively. The qRT-PCR validated the expression profile and revealed the temporal expression patterns of the upregulated genes during gonadal sex differentiation in PBT. qRT-PCR validation targeted key factors in sex steroidogenesis and conservative factors and unreported factors in fish sex differentiation, which were enriched in multiple GO pathways. The expression profiles of genes encoding key enzymes in estrogen and androgen biosynthesis, including *aromatase* and *cyp11c1*, were also validated through *in situ* hybridization (see Supplementary Fig. S3 online; https://doi.org/10.1038/s41598-023-40914-y). Hence, this study provides numerous candidate genes potentially responsible for gonadal sex differentiation in PBT.

The enriched GO terms further characterized the upregulated genes for each sex. The genes upregulated in the females were highly enriched in cell/tissue development-related GO

terms. These genes may be linked to ovarian cavity and lamella formation because somatic cells proliferate in the female gonads to form them during ovarian differentiation (Nakamura et al., 1998; Strüssmann and Nakamura, 2002). We previously established the formation of these structures during ovarian differentiation in PBT (Hayashida et al., 2021). By contrast, several upregulated genes in the males were enriched in structural development-related GO terms. These genes may be linked to the development of a structural framework, namely, the seminiferous epithelium, which is required for spermatogenesis in testes. The seminiferous epithelium is composed of Sertoli and germline cells (Vogl et al., 2000; Batlouni et al., 2009). The Sertoli cells create several junctions to provide developing germ cells with essential structural support (Vogl et al., 2000; Batlouni et al., 2009). Thus, our enrichment analysis disclosed numerous candidate genes responsible for developing ovarian and testicular structures in PBT.

Sex hormones play vital roles in gonadal sex differentiation in fish (Nagahama et al., 2021). In this chapter, we found that the genes upregulated in the males were enriched in steroidogenesis-related GO terms. Furthermore, certain genes encoding key enzymes implicated in gonadal sex steroidogenesis, including *star*, *cyp11a2*, *cyp17a1*, *cyp17a2*, *cyp11c1*, and *hsd11b2*, were upregulated in the males. *Cyp11c1* and *hsd11b2* encode key enzymes in androgen biosynthesis, and qRT-PCR confirmed that they were upregulated in differentiating male

gonads. Our results indicate that androgen biosynthesis is upregulated in male gonads during testicular differentiation in PBT. Exogenous androgens, such as 17-α-methyltestosterone, induce masculinization in various species of fish with female genotype (Budd et al., 2015). However, the roles of endogenous androgens in testicular differentiation in fish are poorly understood. Androgen biosynthesis is absent in differentiating male Nile tilapia gonads (Nakamura et al., 2003; Ijiri et al., 2008). Therefore, endogenous androgens may not be essential for testicular differentiation in this species. In contrast, androgen biosynthesis is upregulated in differentiating male rainbow trout gonads (Liu et al., 2000; Govoroun et al., 2001). Nevertheless, it only occurs after early testicular differentiation (Vizziano et al., 2007). Hence, testicular differentiation may be initiated in the absence of endogenous androgens in this species. In male PBT gonads, *cyp11c1* and *hsd11b2* were upregulated only after the onset of morphological sex differentiation. Li et al. (2019) suggested that endogenous androgens maintain testicular fate by suppressing ovarian differentiation in fish. In PBT, the upregulation of androgen biosynthesis may not directly induce testicular differentiation; rather, it might indirectly promote testicular differentiation by suppressing ovarian differentiation.

Unlike androgens, endogenous estrogens synthesized by Aromatase are essential for ovarian differentiation in fish (Guiguen et al., 2010; Li et al., 2019; Nagahama et al., 2021). In this chapter, comparative transcriptome analysis revealed *aromatase* upregulation in females.

qRT-PCR analysis revealed that the expression of *aromatase* increased specifically in the gonads of genotypic females during sex differentiation in PBT. Our results suggest that Aromatase plays an important role in ovarian differentiation in PBT, as reported in many other fish species (Guiguen et al., 2010; Li et al., 2019; Nagahama et al., 2021).

In this chapter, our comparative transcriptome analysis revealed *foxl2* upregulation in females. This gene is also critical in ovarian differentiation, which regulates the *aromatase* transcription either by directly binding its promoter or interacting with nuclear receptor subfamily 5 group A member 1 (Nr5a1) (Guiguen et al., 2010; Li et al., 2019; Nagahama et al., 2021). qRT-PCR analysis disclosed that *foxl2* was upregulated mainly in differentiating female gonads. Notably, both *foxl2* and *aromatase* were more highly upregulated in females than in males at the morphologically sex-undifferentiated stage. Similar to prior reports on other fish species (Guiguen et al., 2010; Li et al., 2019), our results suggested that Foxl2 also plays a central role in ovarian differentiation in PBT by upregulating *aromatase*. Furthermore, downregulation of the genes controlling testicular differentiation was observed in *foxl2*-knockout genotypic female Nile tilapia (Zhang et al., 2017). Foxl2 may also contribute to ovarian differentiation in PBT by suppressing genes regulating testicular differentiation.

We isolated two genes from the *foxl2* family in the PBT genome, *foxl2* (*foxl2a*) and *foxl3* (*foxl2b*; contig No. g15820). *Foxl3*, a paralog of *foxl2*, is essential for female germ cell

fate decisions in medaka (Nishimura et al., 2015) and Nile tilapia (Dai et al., 2021). In this chapter, comparative transcriptome analysis detected no *foxl3* expression in both sex PBT gonads at the sex-differentiated stage. Furthermore, no differences in germ cell development-related gene expression, including *vasa* (contig No. g25316), *dead end* (contig No. g24023), *nanos1* (contig No. g6249 and g10448), *nanos2* (contig No. g7592 and 7600), *sycp3* (synaptonemal complex protein 3; contig No. g29093), and *dmc1* (DNA meiotic recombinase 1; contig No. g15865) between sexes were observed (see Supplementary Table S1 and 3 online). Our previous analysis revealed that PBT germ cells develop in a sexually dimorphic manner after sex differentiation: germ cell proliferation and differentiation occur earlier in the ovaries than in testes (Hayashida et al., 2021). Gene expressions in germ cells inducing sexual dimorphic development are expected to occur after gonadal sex differentiation in PBT. Notably, two contigs were predicted as genes encoding *nanos1* and *nanos2* from the updated PBT genome. In contrast, no contig was predicted as *nanos3*. Further studies are required to understand the existence of nanos family genes in the PBT genome.

20β-HSD plays a pivotal role in final oocyte maturation by producing MIH, i.e., 17α, 20β-dihydroxy-4-pregnen-3-one (Young et al., 2005; Rajakumar and Senthilkumaran, 2020). In our comparative transcriptome analysis, no *hsd20b2* expression was detected in either sex. This is a reasonable result because no oocytes were observed in the sex-differentiated-stage PBT

ovaries subjected to RNA-Seq.

The transcription factor Dmrt1 is implicated in vertebrate testicular differentiation (Nagahama et al., 2021). Furthermore, Gsdf promotes testicular differentiation in fish (Nagahama et al., 2021). Our comparative transcriptome analysis identified *dmrt1* and *gsdf* upregulation in male PBT. qRT-PCR analysis revealed that *dmrt1* and *gsdf* were upregulated in male gonads during testicular differentiation. These results and our understanding of the important roles of Dmrt1 and Gsdf in fish testicular differentiation (Nagahama et al., 2021) suggest that Dmrt1 and Gsdf regulate this developmental process in PBT.

AMH signaling comprises Amh and its receptor Amhr2, and it has a vital function in testicular differentiation in several fish species (Nagahama et al., 2021). Furthermore, several studies have suggested that Sox9s (two types of *sox9* genes are found in fish, namely, *sox9a* and *sox9b* (or *sox9a2*), because of teleost-specific genome duplication (Klüver et al., 2005), whereas mammals possess only a single copy of *sox9*) may participate in gonadal sex differentiation in fish (Vizziano et al., 2007; Wei et al., 2016). Nevertheless, our comparative transcriptome analysis showed that *amh*, *amhr2*, *sox9a*, and *sox9b* were expressed at the same levels in both sexes. AMH signaling and Sox9s are generally regarded as gonadal development factors and sex differentiation regulators in fish (Nagahama et al., 2021). In PBT, these factors may be involved in ovarian and testicular development rather than gonadal sex differentiation.

In fish gonads, sexually dimorphic expression of the genes regulating sex differentiation generally occurs before morphological sex differentiation (Nagahama et al., 2021). This study confirmed *aromatase* and *foxl2* upregulation in female PBT gonads at the morphologically sex-undifferentiated stage (41 dph). By that time, gonadal sex differentiation had already been initiated at the gene expression level. In contrast, the expression levels of *dmrt1* and *gsdf* did not differ between the sexes at this stage. We speculate that Foxl2 and Aromatase trigger ovarian differentiation, whereas Dmrt1 and Gsdf are not required for triggering testicular differentiation. However, they are vital for promoting testicular differentiation. Incidentally, our qRT-PCR analysis identified upregulation of *cldn11a* in male PBT gonads at the morphologically sex-undifferentiated stage (41 dph). In mice, *claudin 11* is expressed in Sertoli cells and is an obligatory protein for forming tight junctions in testis (Mazaud-Guittot et al., 2010). *Cldn11a* may be an upstream factor that initially induces testicular differentiation in fish. To the best of our knowledge, this is the first report on the relationship between *cldn11a* and early gonadal sex differentiation in fish. This gene will be studied in detail in the future.

We recently identified a male-specific homolog of *sult1st6*, namely *sult1st6y*, as a candidate sex-determining gene in PBT (Nakamura et al., 2021). Our comparative transcriptome analysis revealed *sult1st6y* upregulation in males. Furthermore, qRT-PCR analysis revealed

specific upregulation of *sult1st6y* in male gonads during testicular differentiation. Sulfotransferases deactivate endogenous estrogens by sulfating them (Negishi et al., 2001). In zebrafish, Sult1st6 displays strict substrate specificity for estrogens (Yasuda et al., 2005). We speculated that Sult1st6y would trigger testicular differentiation through estrogen deactivation in male gonads at the onset of gonadal sex differentiation (Nakamura et al., 2021), and estrogen deficiency induces upregulation of the genes promoting testicular differentiation, particularly *dmrt1* and *gsdf*. We are currently investigating the mechanism by which Sult1st6y deactivates estrogens.

In conclusion, we have developed a global gene expression profile for gonadal sex differentiation in PBT using NGS technology. Based on our findings, we propose that ovarian differentiation is mainly induced by Aromatase and Foxl2, whereas Dmrt1 and Gsdf play central roles in testicular differentiation in PBT. Furthermore, Sult1st6y might play a critical role in triggering testicular differentiation. We have previously demonstrated the morphological characteristics of gonadal sex differentiation in PBT (chapter 2; Hayashida et al., 2021). The discoveries made in the previous and current chapters lay the theoretical and empirical foundations for developing sex manipulation technologies for PBT.

Chapter 4.

First data on sexual dimorphic growth of cultured Pacific bluefin tuna, *Thunnus orientalis* (Temminck et Schlegel), and its sex manipulation by treatment with an aromatase inhibitor

Introduction

Tuna (genus *Thunnus*) are commercially important fish in the global aquaculture industry (Naylor and Burke, 2005). Pacific bluefin tuna (*T. orientalis*; PBT) specifically, due to its high market value, is one of the most important species for aquaculture worldwide (Masuma et al., 2011). Currently, several research institutes and companies in Japan have achieved closed-cycle production of this species (Sawada et al., 2005; Masuma et al., 2011), and have made hatchery-produced tuna seed available for practical tuna aquaculture (Murashita et al., 2021; Okada et al., 2021). However, most bluefin tuna aquaculture practices rely on wild-caught juveniles for seed stocks owing to the low productivity of closed-cycle aquaculture (Higuchi et al., 2018; Ienaga et al., 2022). There are numerous issues associated with the use of wild-caught juveniles for aquaculture, including the unstable supply and the negative impacts on wild stock management (Masuma et al., 2011). Because PBT are endangered, due to overfishing of wild stocks, the fishing of this species is currently controlled based on an assessment by the Western and Central Pacific Fisheries Commission (WCPFC). Promotion of closed-cycle aquaculture is necessary for species conservation and sustainable development of the tuna farming industry (Sawada et al., 2013); however, this requires the development of technology that improves its productivity.

The exhibition of sexual dimorphism in growth performance is common in fishes, with some species exhibiting superior female growth and others exhibiting superior male growth (Budd et al., 2015; Mei and Gui, 2015). For example, male tilapia (*Oreochromis niloticus*) grows to a larger size than females (Hanson et al., 1983), whereas female barfin flounder (*Verasper moseri*) grows to a

larger size than males (Mori et al., 1999). Due to these patterns of sexually dimorphic growth, mono-sex production is a desirable technology for the aquaculture industry, as it can help improve productivity by shortening production times and reducing production costs (Budd et al., 2015). In addition, mono-sex stocks can also have other beneficial effects in aquaculture, such as preventing unwanted reproduction, reducing aggressive interactions, and improving the dress-out percentage and body coloration at harvest (Beardmore et al., 2001; Lutz 2001; Budd et al., 2015).

To the best of our knowledge, body size measurement data of cultured tuna at harvest for each sex has only been obtained by Sawada et al. (2013), and detailed data regarding the sex-wise growth performance of tuna species in aquacultural settings are limited. Previous studies reported that in wild stocks of PBT, males tend to be larger than females (Shimose et al., 2009; Shiao et al., 2017). A similar tendency has also been reported in several tuna species, including the Atlantic bluefin tuna (*T. thynnus*) (Hurley and Iles, 1983), southern bluefin tuna (*T. maccoyii*) (Gunn et al., 2008), bigeye tuna (*T. obesus*) (Farley et al., 2006), and albacore (*T. alalunga*) (Chen et al., 2012). These findings potentially suggest that in tuna species, males also exhibit higher growth performance than females in aquacultural settings. Long periods of time (approximately more than 3 years) and huge economic costs are required to rear PBT until harvest size (Sawada et al., 2013; Endo et al., 2016). If male cultured PBT exhibits higher growth performance than females, the production of mono-sex male stocks will be a prominent tool for significantly improving the productivity of closed-cycle PBT aquaculture by shortening production times and reducing production costs.

Sex steroid hormones play a critical role in fish sex differentiation (Yamamoto, 1969).

Therefore, sex manipulation in fish can be achieved via exogenous administration of sex steroids, such as 17β-estradiol (estrogen) and 17α-methyltestosterone (androgen) (Pandian and Sheela, 1995; Guiguen et al., 2010; Budd et al., 2015; Li et al., 2019). Apart from sex steroids, aromatase inhibitors (AIs)—such as fadrozole—are commonly used to induce masculinization in fish (Budd et al., 2015). Androgens are converted to estrogens through a reaction catalyzed by cytochrome P450 aromatase (P450-arom; hereafter, aromatase) (Guiguen et al., 2010). During the critical period of molecular sex differentiation in fish, Aromatases and endogenous estrogens are expressed and synthesized specifically in the female gonads and act as inducers of ovarian differentiation (Guiguen et al., 2010; Li et al., 2019). Aromatase inhibitors work by irreversibly deactivating the Aromatase enzyme and suppressing estrogen synthesis in female gonads, resulting in sex reversal of genotypic females into phenotypic males (Budd et al., 2015).

Fish are highly sensitive to the effects of exogenous sex steroids or AI during the labile period, when the gonads are undifferentiated (Yamamoto, 1969). Therefore, the administration of exogenous sex steroids or AI should be initiated prior to gonadal sex differentiation. Moreover, carefully selecting the method of administration is important for the development of mono-sex production technology, as sex manipulation efficiency, cost-effectivity, and usability depend on the method (Budd et al., 2015). Sex steroids or AI can be administered through several routes, including direct injection of the agent into the muscle or body cavity of the fish, direct immersion of the fish into culture water containing the agent, or oral delivery via incorporation into the feed (Crim, 1985). Administering exogenous sex steroids or AI via dietary supplementation is one of the most common

approaches for sex manipulation in aquaculture due to its simplicity of administration and applicability at a commercial scale (Budd et al., 2015). As such, this method has been proven to be an effective strategy for producing 100% mono-sex stocks (Nakamura and Takahashi, 1973; Nakamura, 1975; Chatain et al., 1999; Budd et al., 2015).

As shown in chapter 3, we revealed that the expression of *aromatase* increases specifically in the gonads of genotypic females during sex differentiation in PBT, suggesting that Aromatase plays an important role in ovarian differentiation in this fish (Hayashida et al., 2023a), consistent with reports in many other fish species (Guiguen et al., 2010; Li et al., 2019). In cases where estrogen synthesis by Aromatase is essential for ovarian differentiation, the suppression of Aromatase activity would be effective in inducing sex reversal of genotypic females into phenotypic males in PBT.

The objective of this study was to investigate sexual dimorphism in the growth performance of PBT in aquacultural settings and develop a technique for its sex manipulation, for the first time in tuna species. First, we compared the body sizes of aquaculture-produced PBTs at harvest between sexes. Additionally, as a first step toward establishing mono-sex male PBT production technology, we orally administered AI into juvenile PBT during the labile period, when the gonads differentiate (Hayashida et al., 2021). We used letrozole—a third-generation non-steroidal AI with high specificity and potency to Aromatase compared with other AIs (Bhatnagar, 2007)—since successful and effective masculinization by letrozole treatment has been reported in several marine fish species, including dusky grouper (*Epinephelus marginatus*) (Garcia et al., 2013), blue drum (*Nibea mitsukurii*), and yellow drum (*N. albiflora*) (Qin et al., 2020). Our results provide the basis for

future studies on the development and establishment of technologies for mono-sex male production in PBT, which will contribute to the further development of closed-cycle PBT aquaculture and meet conservation objectives for wild PBT stocks. Moreover, this study offers important insights into the understanding of sex-wise growth of tuna species in aquacultural settings and developing techniques for its sex manipulation.

Materials and Methods

Ethics

All experiments were performed in accordance with the Guidelines for the Care and Use of Live Fish of the Fisheries Technology Institute (FTI), Japan Fisheries Research and Education Agency (FRA), and were approved by the Institutional Animal Care and Use Committee of FTI.

Sampling of cultured PBT at harvest

In February and August 2021, we sampled 4-year-old PBTs that had been commercially cultured from wild-caught seedlings in the coastal area of Takashima (Nagasaki, Japan). Wild-caught 1-year-old juveniles were transferred to offshore net cage and reared until 4 years old under natural water temperature and photoperiod conditions. Fish were mainly fed defrosted chub mackerel (*Scomber japonicus*) until harvest. The fishes in the offshore net cage were caught and sacrificed through electroshock. Immediately after harvesting, the gills and guts of the fish were removed, placed on ice, and transported to an onshore facility. The fork length (FL, cm) and body weight (BW, kg) of each fish were measured. The individuals were sexed by visual observation of the dissected gonads, and the gonad weight (GW, g) was measured. The gonads were then fixed with Bouin's solution, stored in 70% ethanol at 4 °C, and processed for histological analysis. Individual gonads were classified into different groups based on their maturity status after histological observation. Briefly, female gonads were categorized into the perinucleolar (oocyte at perinucleolus stage), oil droplet (oocyte at oil droplet stage), early vitellogenic (oocyte at primary and/or secondary yolk

globule stages), and late vitellogenic (oocyte at tertiary yolk globule and/or migratory stages) according to the most advanced type of oocytes found in the females. Male gonads were categorized into the early (spermatogonia and spermatocytes dominant), mid (with spermatogonia, spermatocytes, spermatids, and sperm present), and late (sperm becoming dominant) spermatogenesis stages. The condition factor (CF) and gonad index (GI) were calculated as follows:

$$CF = BW/FL^3 \times 10^5$$

$$GI = GW/FL^3 \times 10^4$$

AI treatment

PBT juveniles reared from fertilized eggs at Nagasaki Prefectural Institute of Fisheries (Nagasaki, Japan) were transferred to Nagasaki Field Station, FTI, FRA (Nagasaki, Japan), and used for AI treatment experiments. In trial 1 (2019), a total of 180 and 80 fish at 31 days post hatching (dph) were grouped into AI-treated (experimental) and non-treated (control) groups, respectively. The TL and BW of PBT juveniles at 31 dph in trial 1 were 3.20 ± 0.04 cm and 0.35 ± 0.01 g, respectively (n = 25 fish, 17 genotypic females and 8 genotypic males; mean ± standard error of the mean, SEM). In trial 2 (2021), a total of 600 and 11,200 fish at 35 dph were grouped into AI-treated (experimental) and control groups, respectively. The TL and BW of PBT juveniles at 35 dph in trial 2 were 4.50 ± 0.06 cm and 0.88 ± 0.06 g, respectively (n = 40 fish, 25 genotypic females and 15 genotypic males; mean ± SEM).

PBT juveniles were reared in 7- and 38-ton indoor tanks with natural seawater during the

experiments. Both groups were fed an artificial diet of Magokoro (Nisshin Feed, Tokyo, Japan) and Ambrosia (FEED ONE, Kanagawa, Japan) to apparent satiety 3–5 times per day. Letrozole (Tokyo Chemical Industry, Tokyo, Japan)—a nonsteroidal AI—was administered at a dose of 100 mg/kg feed (Garcia et al., 2013; Komatsu et al., 2006b) until the end of the experiment (59 dph in trial 1 and 70 dph in trial 2). The photoperiod was fixed at 24 h of light in both trials. The natural seawater was sterilized by exposure to UV before being poured into the rearing tanks. The water temperature, depending on the natural seawater, was in the range of 23.2–27.5 °C in trial 1 and 22.4–26.2 °C in trial 2 during the experimental period. At the end of the experiment, the fish were sampled after being anesthetized with 2-phenoxyethanol. Blood samples were collected using heparinized syringes and kept on ice until centrifugation at 1,500 ×g for 15 min at 4 °C. Following this, the plasma was stored at −30 °C until the measurement of sex steroid levels. The TL (cm) and BW (g) of each sampled fish were measured. The dissected gonads were fixed with Bouin's solution, stored in 70% ethanol at 4 °C, and processed for histological analysis. The phenotypic sex of individuals was determined by the presence of ovarian characteristics (an ovarian cavity with ovarian lamellae) and testicular features (the efferent duct appears as a slit in the stromal tissue with a triangular shape), as reported previously (Hayashida et al., 2021). The blood vessels in gonads appeared to be larger in the ovaries than in the testes during gonadal sex differentiation in PBT (Hayashida et al., 2021). Therefore, the cross-sectional area of the blood vessels in the gonads was measured from digital images using the image analysis software, ImageJ (National Institutes of Health, Bethesda, MD) (Hayashida et al., 2021). Expression levels of sex steroid synthesis- and sex differentiation-related genes (*aromatase*, *cyp11b*,

hsd11b2, *foxl2*, *dmrt1*, and *gsdf*), which have been identified previously (Hayashida et al., 2023a), in sex-reversed PBT gonads were also examined. The dissected gonads were placed in RNAlater (Ambion, Austin, TX), stored at −30 °C, and processed for quantitative real-time reverse transcription PCR (qRT-PCR). The fin or muscle samples of each fish were stored in 300 µl TNES-urea buffer (6 M urea; 10 mM Tris-HCl; pH 7.5; 125 mM NaCl; 10 mM EDTA; 1% SDS) at room temperature according to Asahida et al. (1996), and processed for PCR-based genotypic sex identification (Suda et al., 2019; Hayashida et al., 2021).

Histology

The fixed gonads were dehydrated and embedded using standard paraffin embedding methods. The gonads were then cut into 5 µm-thick sections using a microtome (HistoCore BIOCUT, Leica Biosystems, Wetzlar, Germany) and stained with hematoxylin and eosin. The stained sections were imaged and photographed using a light microscope (BX-43, Olympus, Tokyo, Japan) equipped with a digital camera (DP-70, Olympus).

qRT-PCR

Total RNA was extracted using ISOGEN (Nippon Gene, Toyama, Japan) and then treated with TURBO DNase (Ambion) according to the manufacturer's instructions. A 1 µl aliquot of the total RNA was used for quantification with a NanoDrop spectrometer (ND-1000, Thermo Fisher Scientific, Rockford, IL). qRT-PCR was performed as previously described (Hayashida et al., 2023a).

The gene-specific primers and cycling conditions were according to Hayashida et al. (2023a). As the standard for quantification, we used a plasmid containing a partial cDNA sequence of a target gene. The standard sets of seven points ranged from 1×10^8 to 1×10^2 copies and were prepared by 10 × serial dilutions. Technical duplicates were performed for all experimental samples and standards.

Sex steroid measurement

Sex steroid measurements were performed as described by Higuchi et al. (2021). Briefly, steroids were extracted from 100 µl of plasma with dimethyl ether, which was then evaporated. The dried extracts were reconstituted in an assay buffer (ELISA buffer, Cayman Chemical, Ann Arbor, MI). The plasma levels of E2 and 11-KT were analyzed with an enzyme-linked immunosorbent assay (ELISA) using the commercially available Estradiol ELISA kit and Testosterone 11-Keto-EIA kit, respectively (Cayman Chemical). The intra-assay CV was determined by repeated measurements (n = 7) of standard plasma samples from the same plate. For the E2 and 11-KT assays, the intra-assay CV was 13.31% and 10.05%, respectively.

Statistical analysis

Data are presented as the mean ± SEM. We tested for differences in the FL, BW, CF, and GI of harvested PBTs at each sampling period between the sexes using Welch's t-test ($P < 0.05$). Significant differences in the TL, BW, gonadal blood vessel area, plasma sex steroid levels, and gene expression levels of PBTs in the AI treatment experiment were tested by a two-way ANOVA followed

by Tukey's multiple comparison test. Statistical analyses were performed using Prism 7.0 (GraphPad Software, San Diego, CA).

Results

Sexual dimorphism in growth performance of cultured PBT at 4 years old

The FL, BW, BW including GW, CF, GI, and maturity status of cultured PBTs of both sexes at 4 years of age are listed in Table 4.

In February 2021 (n = 50 females and 47 males), there were no significant differences in the FL, BW, BW including GW, and CF between the sexes ($P > 0.05$). The GI was significantly higher in females than in males ($P < 0.05$). During this period, the ovaries of all females were in the pre-vitellogenic stage (perinucleolar and oil droplet stages). Similarly, all males had testes at the early- and mid-spermatogenesis stages.

In August 2021 (n = 24 females and 40 males), the FL and BW values of males were significantly higher than those of females ($P < 0.05$). The BW including GW of males tended to be larger than that of females, although there was no significant difference ($P > 0.05$). There was no significant difference in the CF between the sexes ($P > 0.05$). The GI was significantly higher in females than in males ($P < 0.05$). During this period, approximately 70% of females and 60% of males had reached sexual maturation (late vitellogenic stage in females and late spermatogenesis stage in males).

Table 4. Fork length, body weight, condition factor, gonad index, and maturity status of cultured Pacific bluefin tuna at 4 years old for each sex.

Sampling period	Sex*	No. of sampled fish	Fork length (cm)**	Body weight (kg)**	Body weight including gonad weight (kg)**	Condition factor**	Gonad index**	Gonadal developmental stage***						
								PN (%)	OD (%)	EVG (%)	LVG (%)	ESG (%)	MSG (%)	LSG (%)
February 2021	Female	50	144.64 ± 0.68[a]	51.34 ± 0.70[a]	51.50 ± 0.66[a]	1.69 ± 0.01[a]	0.75 ± 0.02[a]	42 (84.0)	8 (16.0)	0	0	-	-	-
	Male	47	144.78 ± 0.81[a]	51.35 ± 0.79[a]	51.40 ± 0.79[a]	1.68 ± 0.01[a]	0.15 ± 0.00[b]	-	-	-	-	35 (74.5)	12 (25.5)	0
August 2021	Female	24	155.58 ± 1.00[A]	63.54 ± 1.69[A]	64.95 ± 1.77[A]	1.68 ± 0.02[A]	3.82 ± 0.66[A]	3 (12.5)	1 (4.2)	3 (12.5)	17 (70.8)	-	-	-
	Male	40	158.80 ± 1.15[B]	68.69 ± 1.83[B]	69.36 ± 1.82[A]	1.70 ± 0.02[A]	1.76 ± 0.22[B]	-	-	-	-	0	15 (37.5)	25 (62.5)

* Sex of individuals was identified by visual observation of gonads. ** Data are presented as the mean ± standard error of the mean (SEM). Different letters indicate significant difference between sexes at the same sampling period ($P < 0.05$, Welch's *t*-test). Body weight of individuals was recorded after being gilled and gutted. Condition factor = body weight (kg) / fork length (cm)^3 × 10^5. Gonad index = gonad weight (g) / fork length (cm)^3 × 10^4. *** Maturity status of gonads is classified into perinucleolus (PN), oil droplet (OD), early vitellogenic (EVG), and late vitellogenic (LVG) stages according to the most advanced type of oocytes found in female, and into early (ESG), mid (MSG), and late spermatogenesis (LSG) stages in male by histological observation of gonads (Higuchi et al., 2021).

Effects of AI treatment on survival, growth, and gonadal development in PBT

The survival, growth, and gonadal development of PBTs of both sexes in the AI-treated and non-treated (control) groups are summarized in Table 5. The survival rate tended to be higher in the AI-treated group than in the control group in both trials. In trial 2, there were no significant differences in TL and BW between the groups ($P > 0.05$). In both trials, the gonadal blood vessel areas of genotypic females in the AI-treated group tended to be smaller (Fig. 10C) than those of genotypic females in the control group (Fig. 10A). The genotypic males in the AI-treated (Fig. 10D) and control (Fig. 10B) groups also showed similar differences in gonadal blood vessel area. In trial 2, the gonadal blood vessel area of genotypic females in the AI-treated group was significantly smaller than that of genotypic females in the control group, as in the case of genotypic males in both AI-treated and control groups ($P < 0.05$) ($n = 4$ fish). In both trials, all individual gonads in the control group had differentiated into ovaries or testes depending on the genotypic sex of the individual (Fig. 10A and B). In contrast, the gonads of genotypic males (Fig. 10D) as well as those of genotypic females (Fig. 10C) in the AI-treated group showed testicular characteristics (the efferent duct appears as a slit in the stromal tissue with a triangular shape).

Table 5. Effects of treatment with an aromatase inhibitor (AI) on the survival, growth, and gonadal development of the Pacific bluefin tuna.

Trial (Year)	Sampling period (dph†)	Treatment	Rearing tank (ton)	Survival rate (%)	Genotype‡	No. of sampled fish	Total length § (cm)	Body weight § (g)	Histological area of gonadal blood vessels § (μm²)	Phenotype¶	
										Female (%)	Male (%)
1 (2019)	59	Control	7	12.00	Female	7	12.31 ± 0.52	21.99 ± 2.61	1159.84 ± 324.00	7 (100)	0
					Male	3	12.09 ± 1.14	22.78 ± 5.33	178.88 ± 63.61	0	3 (100)
		AI	38	23.00	Female	18	13.26 ± 0.23	27.69 ± 1.67	370.26 ± 106.87	0	18 (100)
					Male	2	14.78	37.26	281.25	0	2 (100)
2 (2021)	70	Control	38	2.67	Female	15	14.30 ± 0.18[a]	29.55 ± 1.50[a]	2758.27 ± 638.48[a]	15 (100)	0
					Male	15	14.37 ± 0.15[a]	29.85 ± 1.00[a]	1117.95 ± 306.77[b]	0	15 (100)
		AI	7	12.83	Female	40	14.06 ± 0.15[a]	28.10 ± 1.11[a]	928.12 ± 190.58[b]	0	40 (100)
					Male	37	14.04 ± 0.18[a]	27.15 ± 1.23[a]	613.84 ± 110.08[b]	0	37 (100)

†dph: days post hatching.

‡The genotypic sex of each fish was identified using male-specific DNA markers (Suda et al., 2019).

§ Data are presented as mean ± standard error of the mean. The data of AI-treated genotypic males in trial 1 are presented as mean values ($n = 2$ fish). Two-way ANOVA followed by Tukey's multiple comparison test was performed to determine statistical differences in total length, body weight, and histological area of gonadal blood vessels among groups in trial 2. Different letters indicate significant differences ($P < 0.05$).

¶The phenotypic sex of each fish was identified through the histological observation of gonads (Hayashida et al., 2021).

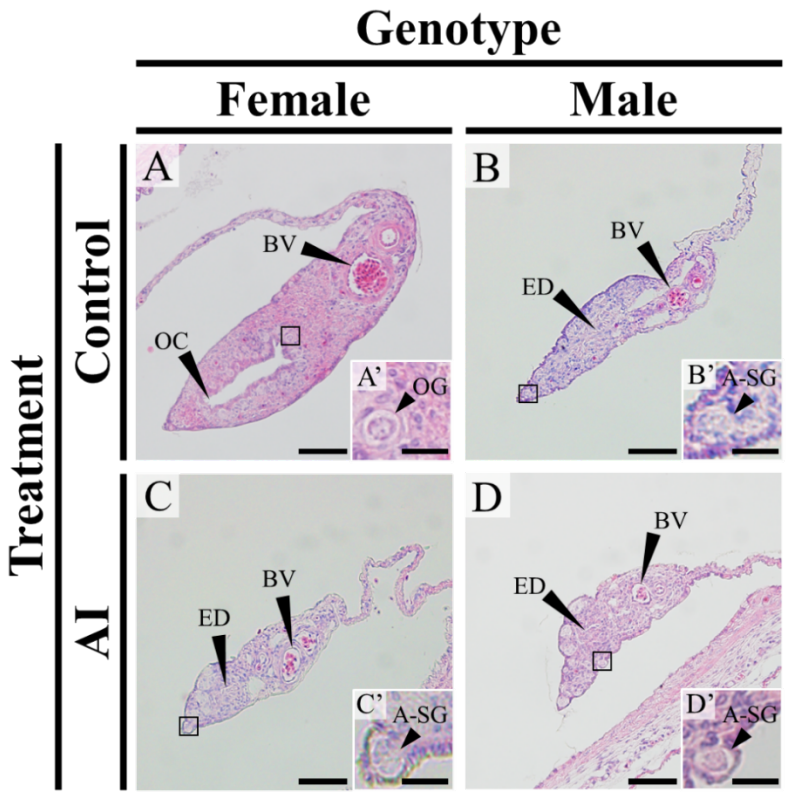

Figure 10. Histological images of the gonads of Pacific bluefin tuna in the aromatase inhibitor (AI)-treated and non-treated (control) groups. Images are shown for each genotypic sex at 70 days post hatching. (A and B) All individual gonads in the control group have differentiated into ovaries or testes depending on the genotypic sex of the individual. (C and D) The gonads of genotypic males as well as those of genotypic females in the AI-treated group show testicular characteristics: smaller gonadal blood vessels, and the efferent duct appears as a slit in the stromal tissue with a triangular shape. Transverse sections of the gonads are stained with hematoxylin and eosin. The genotypic sex of individuals was identified using male-specific DNA markers. The insets show a higher magnification of the area where the germ cells are located. Arrowheads indicate the following: OG, oogonia; A-SG, type-A spermatogonia; OC, ovarian cavity; BV, blood vessels; ED, efferent duct. Bars = 50 μm (A–D) and 10 μm (A'–D').

Sex steroid synthesis- and sex differentiation-related gene expression in sex-reversed gonads

Fig. 11 shows the sex steroid synthesis- and sex differentiation-related gene expression levels in sex-reversed gonads (genotypic female/phenotypic male). *Aromatase* and *foxl2* expression levels were significantly higher in the genotypic/phenotypic females than in the others ($P < 0.05$). *Cyp11c1*, *hsd11b2*, *dmrt1*, and *gsdf* expression levels in the genotypic females/phenotypic males were comparable to those in the genotypic/phenotypic males in both the AI-treated and control groups ($P > 0.05$). Nevertheless, *cyp11c1*, *hsd11b2*, *dmrt1*, and *gsdf* expression levels were significantly lower in the genotypic/phenotypic females than in the others ($P < 0.05$).

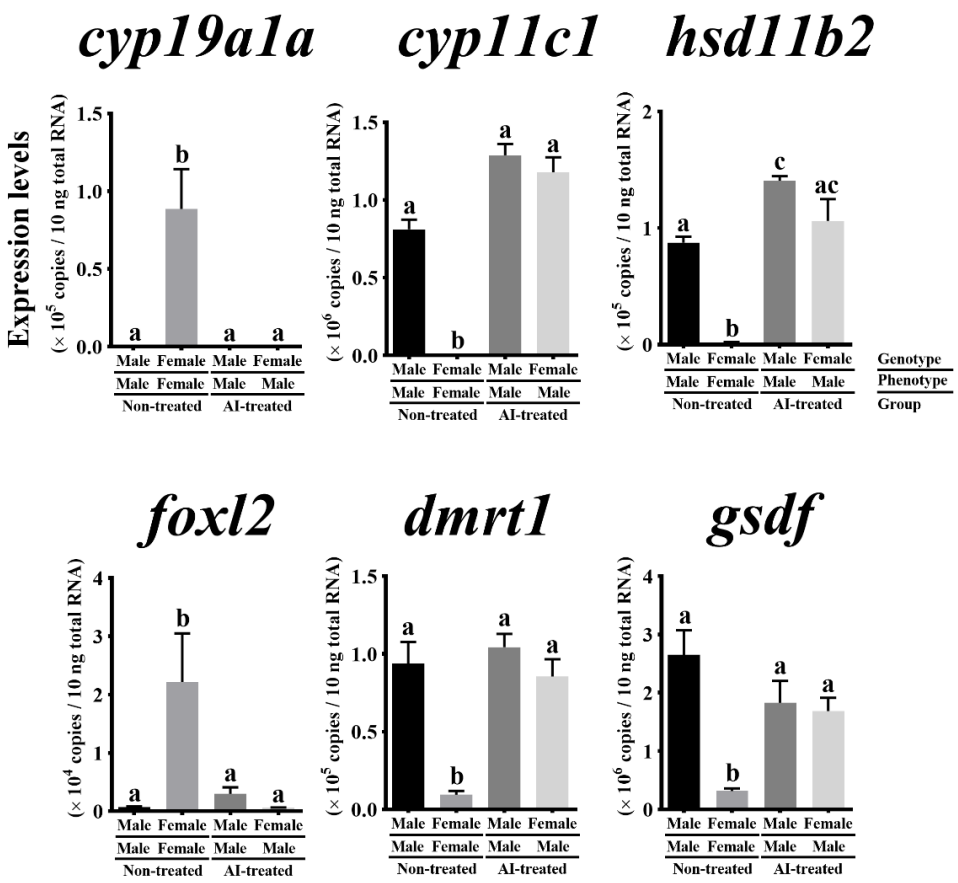

Figure 11. Expression patterns of sex steroid biosynthesis- and sex differentiation-related genes in sex-reversed (genotypic female/phenotypic male) Pacific bluefin tuna gonads. Total RNA extracted from gonads at the morphologically sex-differentiated stage (70 days post-hatching) for each sex genotype in the aromatase inhibitor-treated and untreated control groups were subjected to quantitative real-time reverse transcription PCR. Bars indicate mean ± standard error of the mean (SEM) (n = 3 fish). Different letters indicate significant differences ($P < 0.05$; two-way ANOVA followed by Tukey's multiple comparisons test).

Effects of AI treatment on plasma levels of E2 and 11-KT in PBT

Fig. 12 shows the plasma levels of E2 and 11-KT for each genotypic sex in the AI-treated and control groups in trial 2 (n = 8 fish). Plasma E2 levels tended to be lower in the AI-treated group than in the control group, and were significantly lower in genotypic males in the AI-treated group than in genotypic females in the control group ($P < 0.05$). In both groups, although there were no significant differences ($P > 0.05$), plasma E2 levels tended to be lower in genotypic males than in genotypic females. Plasma 11-KT levels in the AI-treated group were significantly higher than those in the control group ($P < 0.05$). In addition, plasma 11-KT levels of genotypic males were significantly higher than those of genotypic females in both the AI-treated and control groups ($P < 0.05$).

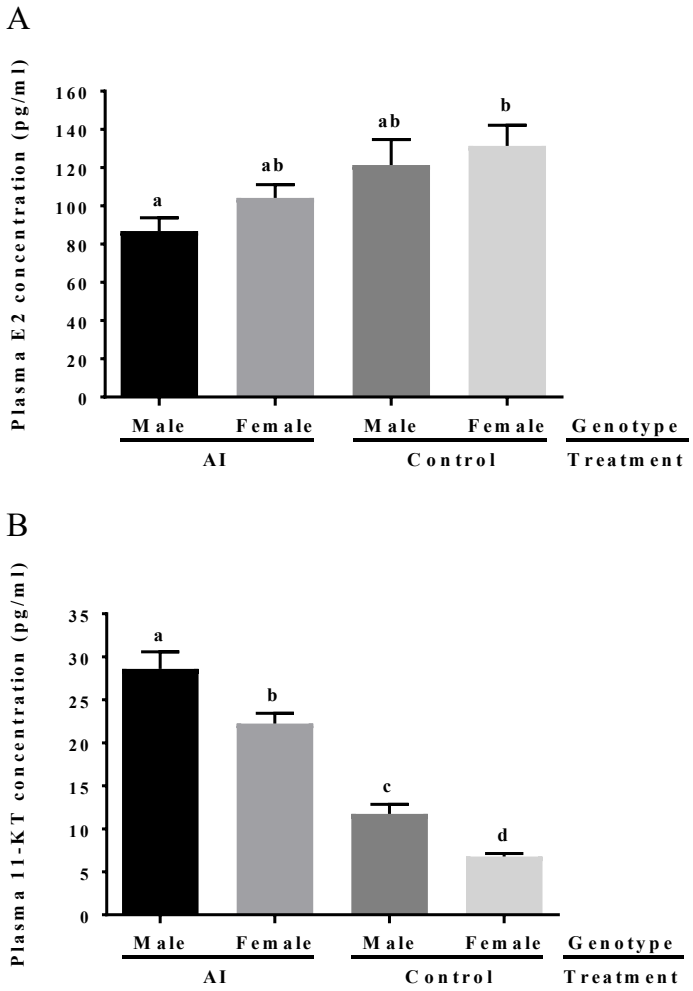

Figure 12. Plasma levels of 17β-estradiol (E2) (A) and 11-ketotestosterone (11-KT) (B) in each genotypic sex of Pacific bluefin tuna in the aromatase inhibitor (AI)-treated and non-treated (control) groups. The genotypic sex of individuals was identified using male-specific DNA markers. Data are presented as the mean ± standard error of the mean (n = 8 fish). Different letters indicate significant differences between group ($P < 0.05$, two-way ANOVA followed by Tukey's multiple comparison test).

Discussion

Sexual dimorphism in growth performance has been confirmed in various aquaculture target species. For this, sex manipulation in fish to produce mono-sex stocks is an important area of aquaculture research (Budd et al., 2015). The present study provides the first data on the sexually dimorphic growth of a tuna species in aquacultural settings and its sex manipulation.

We found that the FL and BW of cultured PBTs at 4 years of age were significantly larger in males than in females during the reproductive season (August 2021). Cultured PBTs, which are reared from wild-caught seedlings, generally reach sexual maturation and stable spawning at 4 years of age (Seoka et al., 2007; Masuma et al., 2011; Gen, 2016). In this chapter, almost all PBTs sampled during the reproductive season had reached sexual maturation. Furthermore, we did not observe any differences in body size between sexes before the fish had reached sexual maturation at 4 years of age (February 2021). Our results suggest that cultured male PBTs exhibit higher growth performance than females at maturity. The most common reason for the higher growth performance of males than females at maturity is that after sexual maturation, females allocate more energy for gonadal maturation and less energy for growth than males (Roff, 1983). Previous studies on wild stocks have reported that several species of tuna—including Atlantic bluefin tuna (Hurley and Iles, 1983), southern bluefin tuna (Gunn et al., 2008), bigeye tuna (Farley et al., 2006), albacore (Chen et al., 2012), and PBT (Shimose et al., 2009)—exhibit size dimorphism between the sexes, with males growing larger than females after reaching maturity. In this chapter, the GI of cultured PBTs during the reproductive season was significantly higher in females than in males, suggesting that females

require more energy for gonadal maturation than males. These results indicate that in cultured PBTs that reach sexual maturity at 4 years of age, sexual dimorphism in growth performance may be due to differences in energy investment for gonadal maturation between the sexes: female PBTs allocate more energy for reproduction after sexual maturation and are thus smaller in body size than males.

Sawada et al. (2013) reported that there is no difference in body size of cultured PBT between sexes until 5 years of age. Although the sample number at each sampling point is unclear, and there are no data available regarding the sexual maturation status of sampled fish in the previous study, it is speculated that the difference in maturation characteristics between hatchery-produced and captive-reared PBTs is one possible cause of the difference in results between Sawada et al. (2013) and this study. Sawada et al. (2013) examined cultured PBTs that were reared from fertilized eggs, while this study examined cultured PBTs from wild-caught seedlings. According to Higuchi et al. (2021), hatchery-produced PBTs seem to have different maturation characteristics from captive-reared PBTs. For instance, all males of hatchery-produced PBTs reach sexual maturation at 3 years of age (Higuchi et al., 2021), while the maturation rate of captive-reared male PBTs at 3–4 years of age is relatively low (20-75 %), as reported by Seoka et al. (2007) and this study. Furthermore, the gonadsomatic index (GSI) of male hatchery-produced PBTs was comparable to or higher than that of females (Higuchi et al., 2021). Sexual dimorphism of growth performance was observed at earlier life stages in this chapter than in previous studies that examined wild stocks, although the data on body size of PBT at this age are limited in previous studies (Shimose et al., 2009; Shiao et al., 2017). Furthermore, our results showed that there was no significant difference in BW including GW

between the sexes at reproductive season of 4 years old (February 2021), although it tended to be larger in males than in females, suggesting that the effect of weight of removed organs, including the gill, gut, and gonad, on the body size of cultured PBT for each sex at harvest needs to be considered for a deeper understanding of the sexual dimorphic growth of PBT in aquacultural settings. To address these issues and completely characterize sexual dimorphic growth of cultured PBT, further data on the growth performance of aquaculture-produced PBTs, including both hatchery-produced and captive-reared PBTs, need to be collected for each sex in future studies.

Our results show that cultured male PBTs exhibit higher growth performance than females, suggesting that mono-sex male production may be a prominent tool for improving the productivity of closed-cycle PBT aquaculture by shortening production times and reducing production costs. Here, we orally administered letrozole, a third-generation non-steroidal AI commonly used in marine aquaculture-target species (Garcia et al., 2013; Qin et al., 2020), into sexually undifferentiated PBT to induce masculinization in genotypic females. Histological analysis revealed that the gonads of all genotypic females in the AI-treated group showed testicular characteristics. Furthermore, we detected high expression levels of *dmrt1* (a key determinant of testicular development) and *cyp11b* (encoding a key enzyme in androgen synthesis) in the sex-reversed gonads of genotypic females, but not in the gonads of genotypic females in the control group. Moreover, serum levels of 11-KT in genotypic females in the AI-treated group were significantly higher than those in genotypic females in the control group. In contrast, *aromatase* expression was not detected in the sex-reversed gonads of genotypic females but was detected in the gonads of genotypic females in the control group.

Furthermore, serum levels of E2 in genotypic females in the AI-treated group tended to be lower than those in genotypic females and even those in genotypic males in the control group. These results indicate that AI administration suppressed the aromatase-catalyzed synthesis of estrogen, resulting in the sex reversal of genotypic females into phenotypic males at the molecular level in PBT.

It is known that the activation of the endogenous sex steroid production pathway is important for maintaining sex-reversed status in fish (Li et al., 2019). In cases of masculinization, endogenous androgen production is critical for maintaining male sex status after a female-to-male sex change, even after treatment with exogenous sex steroids or AI is terminated (Li et al., 2019). In this chapter, the high expression levels of *cyp11b* and high serum levels of 11-KT among genotypic females in the AI-treated group were comparable to those of genotypic males in the control group. These results indicate that the endogenous androgen production pathway in genotypically female PBTs in the AI-treated group was activated to a level comparable to that in genotypic males. Oral administration of AI (letrozole) was reported to induce complete masculinization in rice field eel (*Monopterus albus*): the endogenous androgen production pathway of sexually reversed fish was significantly upregulated compared to that of the non-treated group, the sex-reversed status of AI-treated fish was maintained after cessation of AI treatment, and sexually reversed fish produced functional sperm (Jiang et al., 2022). Sexual fate maintenance after termination of AI treatment was also observed in other fish species, such as Atlantic halibut (*Hippoglossus hippoglossus*) (Babiak et al., 2012), Senegalese sole (*Solea senegalensis*) (Viñas et al., 2013), blue drum, and yellow drum (Qin et al., 2020). Similarly, the reversed sex of genotypically female PBTs may be maintained even when

exogenous AI treatment is terminated.

Several methods have been developed for administering sex steroids and AI, including direct injection, direct immersion, and dietary supplementation (Crim, 1985). However, direct injection is difficult in PBT because it is very difficult to handle this fish, which have extremely delicate skin that can be easily damaged (Endo et al., 2016). Furthermore, PBT juveniles at the stage of gonadal sex differentiation (approximately 40−70 dph) (Hayashida et al., 2021) are generally reared in offshore sea net cages, which helps avoid death due to collision with the walls of the indoor tank in aquaculture operations (Masuma et al., 2011). As such, the administration of sex steroids and AI through direct immersion is not practical in PBT. For these reasons, it is desirable to use an oral administration method for the sex manipulation of PBT in practice. However, this approach is known to have certain limitations. The hormones may degrade during storage or as part of the normal digestion process of the fish (Budd et al., 2015). Moreover, there may be variability in dosage among individuals due to a non-uniform concentration of the hormone in the feed (Budd et al., 2015). Behavioral hierarchies among fish can also influence their feeding rates, leading to differences in the amount of chemicals ingested by the fish (Budd et al., 2015). In this chapter, however, we achieved 100% masculinization of genotypic females via oral administration of AI in both trials. Furthermore, AI treatment did not negatively affect the survival or growth of the fish. Incidentally, other than sex steroid and AI administration, successful masculinization by, for example, temperature treatment during gonadal sex differentiation and cross-species hybridization has been reported (Rahman et al., 2013; Budd et al., 2015). However, it is difficult to perform temperature treatment on PBT juveniles at

the gonadal sex differentiation stage since they are generally reared in offshore sea net cages, as discussed above. Furthermore, it is difficult to perform artificial insemination in mature PBT bloodstocks for producing cross-species hybrids, owing to their large body size and very delicate skin. Hence, our results indicate that oral AI administration is the most effective and practical method for inducing masculinization in genotypically female PBT in aquaculture.

In this chapter, we showed that oral AI administration is effective for inducing sex reversal of PBT from genotypic females to phenotypic males. However, the use of letrozole on aquaculture fish as food is legally restricted, due to potential health risks. Instead of letrozole, therefore, the use of a safer AI is required to establish mono-sex male PBT production systems. Phytochemicals are derived from plants and can potentially be used to inhibit the Aromatase enzyme (Balam et al., 2020). Previously, chrysin (5, 7-dihydroxyflavone), which is a polyphenolic flavonoid with a high concentration in honey and propolis, was reported to have high aromatase inhibitory potency (Dhawan et al., 2002; Balam, et al., 2020). It has been shown that chrysin binds to the active site of Aromatase as a competitive inhibitor regarding substrate (Chen et al., 1997), similar to other AIs including letrozole (Bhatnagar, 2007). Because of the acceptable safety (Kasala et al., 2015), it is expected that oral administration of chrysin would be a practical method to produce mono-sex male stocks in PBT, and this should be tested with priority in future research.

We have previously shown the upregulation of expression of genes encoding key enzymes in estrogen and androgen synthesis during sex differentiation in female and male PBT gonads, respectively (Hayashida et al., 2023a). In this chapter, we observed high serum levels of E2 and 11-

KT in female and male PBTs, respectively, during sex differentiation. Furthermore, this study revealed the crucial role of Aromatase in ovarian differentiation in PBT. The present study provides additional information on the sex differentiation mechanisms of PBT, particularly the role of sex steroid synthesis in this developmental process.

In conclusion, we observed sexual dimorphism in the body size of cultured PBT at harvest, that is, the FL and BW of males were larger than those of females during the reproductive season at 4 years of age. We also found that Aromatase plays a critical role in ovarian differentiation in PBT. Moreover, we demonstrated that sex can be controlled in PBT through the conventional masculinization method, oral AI administration, which resulted in 100% sex reversal of genotypic females into phenotypic males. This study provides a basis for the large-scale production of mono-sex male PBT stocks, which would help improve the productivity of closed-cycle aquaculture of this economically important species by shortening production times and reducing production costs. In fact, according to their high market value based on the market value of aquaculture-produced PBT in Japan (approximately 3,000 yen/kg BW) and the average BW of each sex obtained in this chapter, it is calculated that mono-sex male PBT production will result in a significant increase in aquaculture profits compared with a conventional sex-mixed production system (approximately 10% increase at the reproductive season of 4 years old). Moreover, production of mono-sex male stocks may also be effective in avoiding the deterioration of flesh quality in aquaculture-produced PBT since we recently revealed that the reduction of muscle fat content associated with sexual maturation occurs more frequently in females than in males at maturity (Higuchi et al., unpublished data). The authors

acknowledge that further studies for completely characterizing the sexually dimorphic growth of cultured PBT and demonstrating the gonadal development and growth performance of AI-treated PBTs until adulthood are needed. In addition, further examination to reveal survival performance of AI-treated PBTs is important, since the survival rate of AI-treated groups tended to be higher than that of the non-treated group in both trials. If AI-treated PBTs show higher survival performance at early developmental stages, mono-sex male PBT aquaculture will also be meaningful in the context of efficient fingerling PBT production.

Our results can be further applied to the development of techniques to induce sex reversal of genotypic males to phenotypic females. An increase in female ratios in aquaculture populations via artificial sex manipulation also seems to be important in improving the productivity of closed-cycle PBT aquaculture. Namely, female-rich broodstock management allows for large amounts of high-quality fertilized eggs to be obtained. In addition, sex manipulation techniques have been widely used as powerful tools to elucidate sex determination and differentiation mechanisms in fish (Guiguen et al., 2010; Li et al., 2019). Therefore, the masculinization technique established in this chapter will also be valuable for ongoing investigations focused on sex determination and differentiation in PBT.

Chapter 5.

Summary and conclusion

In chapter 2 (Hayashida et al., 2021), we identified the timing and process of gonadal sex differentiation in PBT. Gonadal sex differentiation in PBT was first histologically characterized by the formation of ovarian cavity in females and an efferent duct in males at 57 dph. The gonads were then directly differentiated into ovaries or testes according to the genotypic sex until 83 dph. During early sex differentiation (41−57 dph), no sexual dimorphic proliferation of germ cells was observed, suggesting that germ cell proliferation may not affect gonadal sex differentiation in PBT.

In chapter 3 (Hayashida et al., 2023a), we identified the molecular mechanism that regulates gonadal sex differentiation in PBT. Based on comparative and temporal transcriptomic analyses, we propose that active Aromatase-mediated estrogen biosynthesis, which includes positive regulation of *aromatase* expression by Foxl2, induces ovarian differentiation in PBT. In contrast, Dmrt1 and Gsdf mainly promote testicular differentiation in PBT. Furthermore, *sult1st6y*, a male-specific homolog of estrogen sulfotransferase, is specifically expressed in male PBT gonads during testicular differentiation. We speculated that Sult1st6y would trigger testicular differentiation through estrogen deactivation in male gonads at the onset of gonadal sex differentiation, and estrogen deficiency induces the upregulation of the genes promoting testicular differentiation, particularly *dmrt1* and *gsdf*. Furthermore, androgen biosynthesis is upregulated in differentiating male gonads, suggesting that endogenous androgens may also be

vital for testicular differentiation.

In chapter 4 (Hayashida et al., 2023b), we further investigated sexual dimorphism in the growth performance of aquaculture-produced PBT and developed techniques for its sex manipulation. A comparison of the body size between the sexes revealed that male-cultured PBTs were larger than females at harvest, suggesting that mono-sex male production may be a prominent tool for improving the productivity of closed-cycle PBT aquaculture by shortening production times and reducing production costs. Furthermore, based on the findings of this study, we demonstrated that sex can be controlled in PBT through the oral AI administration to sexually undifferentiated fish, which resulted in 100% sex reversal of genotypic females into phenotypic males.

In conclusion, this study for the first time shows the comprehensive mechanisms underlying gonadal sex differentiation, superior growth performance of males compared to that of females in aquaculture settings, and the development of an all-male production technique in PBT. This study offers important insights into the establishment of mono-sex male aquaculture in PBT. In addition, the discoveries made herein provide theoretical and empirical foundations for understanding sex differentiation mechanisms in tuna species.

References

Agawa, Y., Iwaki, M., Komiya, T., Honryo, T., Tamura, K., Okada, T., Yagishita, N., Kobayashi, T., Sawada, Y. Identification of male sex-linked DNA sequence of the cultured Pacific bluefin tuna *Thunnus orientalis*. Fish. Sci. 2015, 81, p. 113–121.

Asahida, T., Kobayashi, T., Saitoh, K., Nakayama, I. Tissue preservation and total DNA extraction from fish stored at ambient temperature using buffers containing high concentration of urea. Fish. Sci. 1996, 62, p. 727–730.

Babiak, J., Babiak, I., Nes, S., Harboe, T., Haugen, T., Norberg, B. Induced sex reversal using an aromatase inhibitor, Fadrozole, in Atlantic halibut (*Hippoglossus hippoglossus* L.). Aquaculture 2012, 324–325, p. 276–280.

Balam, F.H., Ahmadi, Z.S., Ghorbani, A. Inhibitory effect of chrysin on estrogen biosynthesis by suppression of enzyme aromatase (CYP19): A systematic review. Heliyon 2020, 6, e03557.

Batlouni, S.R., Nóbrega, R.H., França, L.R. Cell junctions in fish seminiferous epithelium. Fish Physiol. Biochem. 2009, 35, p. 207–217.

Beardmore, J.A., Mair, G.C., Lewis, R.I. Monosex male production in finfish as exemplified by tilapia: applications, problems, and prospects. Aquaculture 2001, 197, p. 283–301.

Bhatnagar, A.S. The discovery and mechanism of action of letrozole. Breast Cancer Res. Treat.

2007, 105, p. 7–17.

Budd, A.M., Banh, Q.Q., Domingos, J.A., Jerry, D.R. Sex control in fish: approaches, challenges and opportunities for aquaculture. J. Mar. Sci. Eng. 2015, 3, p. 329–355.

Chatain, B., Saillant, E., Peruzzi, S. Production of monosex male populations of European seabass, *Dicentrarchus labrax* L. by use of the synthetic androgen 17α-methyldehydrotestosterone. Aquaculture 1999, 178, p. 225–234.

Chen, K.-S., Shimose, T., Tanabe, T., Chen, C.-Y., Hsu, C.-C. Age and growth of albacore *Thunnus alalunga* in the North Pacific Ocean. J. Fish Biol. 2012, 80, p. 2328–2344.

Chen, S., Kao, Y.-C., Laughton, C.A. Binding characteristics of aromatase inhibitors and phytoestrogens to human aromatase. J. Steroid Biochem. Mol. Biol. 1997, 61, p. 107–115.

Crim, L.W. “Methods for acute and chronic hormone administration in fish”. Reproduction and Culture of Milkfish. Lee, C.S. and Liao, I.C. eds. Tungkang, Oceanic Institute and Tungkang Marine Laboratory, 1985, p. 1–13.

Dai, S., Qi, S., Wei, X., Liu, X., Li, Y., Zhou, X., Xiao, H., Lu, B., Wang, D., Li, M. Germline sexual fate is determined by the antagonistic action of *dmrt1* and *foxl3/foxl2* in tilapia. Development 2021, 148, dev199380.

Devlin, R.H. and Nagahama, Y. Sex determination and sex differentiation in fish: an overview of genetic, physiological, and environmental influences. Aquaculture 2002, 208, p. 191–364.

Dhawan, K., Kumar, S., Sharma, A. Beneficial effects of chrysin and benzoflavone on virility in 2-year-old male rats. J. Med. Food 2002, 5, p. 43–48.

Endo, T., Ishida, M., Yazawa, R., Takeuchi, Y., Kumakura, N., Hara, T., Adachi, S. Mass production of fertilized eggs by artificial insemination from captive-reared Pacific bluefin tuna (*Thunnus orientalis*). Aquaculture 2016, 451, p. 72–77.

Farley, J.H., Clear, N.P., Leroy, B., Davis, T.L.O., McPherson, G. Age, growth and preliminary estimates of maturity of bigeye tuna, *Thunnus obesus*, in the Australian region. Mar. Freshw. Res. 2006, 57, p. 713–724.

Felip, A., Zanuy, S., Carrillo, M., Piferrer, F. Induction of triploidy and gynogenesis in teleost fish with emphasis on marine species. Genetica 2001, 111, p. 175–195.

Garcia, C.E.de O., Araújo, B.C., Mello, P.H., Narcizo, A.de M., Rodrigues-Filho, J.A., Medrado, A.T., Zampieri, R.A., Floeter-Winter, L.M., Moreira, R.G. Involvement of pituitary gonadotropins, gonadal steroids and breeding season in sex change of protogynous dusky grouper, *Epinephelus marginatus* (Teleostei: Serranidae), induced by a non-steroidal aromatase inhibitor. Gen. Comp. Endocrinol. 2013, 192, p. 170–180.

Ge, S.X., Son, E.W., Yao, R. iDEP: an integrated web application for differential expression and pathway analysis of RNA-Seq data. BMC Bioinform. 2018, 19, 534. Accessed 24 August 2022.

Gen, K. “Physiology of bluefn tuna reproduction: new insights into reproduction in wild and captive bluefn tuna species”. Biology and Ecology of Bluefn Tuna. Kitagawa, T. and Kimura, S. eds. Boca Raton, FL, CRC Press, 2016, p. 325–354.

Govoroun, M., McMeel, O.M., D'Cotta, H., Ricordel, M.-J., Smith, T., Fostier, A., Guiguen, Y. Steroid enzyme gene expressions during natural and androgen-induced gonadal differentiation in the rainbow trout, *Oncorhynchus mykiss*. J. Exp. Zool. 2001, 290, p. 558–566.

Grier, H.J. Cellular organization of the testis and spermatogenesis in fishes. Am. Zool. 1981, 21, p. 345–357.

Guiguen, Y., Fostier, A., Piferrer, F., Chang, C.-F. Ovarian aromatase and estrogens: A pivotal role for gonadal sex differentiation and sex change in fish. Gen. Comp. Endocrinol. 2010, 165, p. 352–366.

Gunn, J.S., Clear, N.P., Carter, T.I., Rees, A.J., Stanley, C.A., Farley, J.H., Kalish, J.M. Age and growth in southern bluefin tuna, *Thunnus maccoyii* (Castelnau): Direct estimation from otoliths, scales and vertebrae. Fish. Res. 2008, 92, p. 207–220.

Hamaguchi, S. A light- and electron-microscopic study on the migration of primordial germ cells in the teleost, *Oryzias latipes*. Cell Tissue. Res. 1982, 227, p. 139–151.

Hanson, T.R., Smitherman, R.O., Shelton, W.L., Dunham, R.A. “Growth comparisons of

monosex tilapia produced by separation of sexes, hybridization, and sex reversal". Proceedings of the First International Symposium on Tilapia in Aquaculture. Fishelson, L. and Yaron, Z. eds. Nazareth, Tel Aviv University, 1983, p. 570–579.

Hayashida, T., Soma, S., Nakamura, Y., Higuchi, K., Kazeto, Y., Gen, K. Transcriptome characterization of gonadal sex differentiation in Pacific bluefin tuna, *Thunnus orientalis* (Temminck et Schlegel). Sci. Rep. 2023a, 13, 13867.

Hayashida, T., Higuchi, K., Okita, K., Kazeto, Y., Hamasaki, M., Yoshikawa, S., Takashi, T., Gen, K. First data on sexual dimorphic growth of cultured Pacific bluefin tuna, *Thunnus orientalis* (Temminck et Schlegel), and its sex manipulation by treatment with an aromatase inhibitor. Aquac. Res. 2023b, 2023, 1590646.

Hayashida, T., Higuchi, K., Hashimoto, H., Kazeto, Y., Eba, T., Yoshikawa, S., Goto, R., Okita, K., Takashi, T., Ishii, K., Yamashita, T., Kumon, K., Gen, K. Gonadal sex differentiation and early ovarian/testicular development in cultured Pacific bluefin tuna, *Thunnus orientalis* (Temminck et Schlegel). Theriogenology 2021, 173, p. 56–63.

Higuchi, K., Goto, R., Konishi, J., Ina, Y., Kazeto, Y., Gen, K. Early development of primordial germ cells in Pacific bluefin tuna *Thunnus orientalis*. Theriogenology 2019, 131, p. 106–112.

Higuchi, K., Suzuki, A., Eba, T., Hashimoto, H., Kumon, K., Morioka, T., Shiozawa, S., Soma,

S., Okita, K., Takashi, T., Gen, K. Seasonal changes and endocrine regulation of gonadal development in hatchery-produced Pacific bluefin tuna *Thunnus orientalis* broodstock in sea cages. Aquaculture 2021, 545, 737199.

Higuchi, K., Yoshikawa, S., Masaomi, H., Baba, K., Sakurai, K., Norita, T., Miyagishima, S., Yamashita, S., Takashi, T., Gen, K., Oka, M. Relationship between survival and body-size of age-0 Pacific bluefin tuna *Thunnus orientalis* reared from eggs in sea net cages during winter. Aquac. Sci. 2018, 66, p. 147–153. (in Japanese with English abstract)

Howe, K.L., Achuthan, P., Allen, J., Allen, J., Alvarez-Jarreta, J., Amode, M.R., Armean, I.M., Azov, A.G., Bennett, R., Bhai, J., Billis, K., Boddu, S., Charkhchi, M., Cummins, C., Fioretto, L.D.R., Davidson, C., Dodiya, K., Houdaigui, B.E., Fatima, R., Gall, A., Giron, C.G., Grego, T., Guijarro-Clarke, C., Haggerty, L., Hemrom, A., Hourlier, T., Izuogu, O.G., Juettemann, T., Kaikala, V., Kay, M., Lavidas, I., Le, T., Lemos, D., Martinez, J.G., Marugán, J.C., Maurel, T., McMahon, A.C., Mohanan, S., Moore, B., Muffato, M., Oheh, D.N., Paraschas, D., Parker, A., Parton, A., Prosovetskaia, I., Sakthivel, M.P., Salam, A.I.A., Schmitt, B.M., Schuilenburg, H., Sheppard, D., Steed, E., Szpak, M., Szuba, M., Taylor, K., Thormann, A., Threadgold, G., Walts, B., Winterbottom, A., Chakiachvili, M., Chaubal, A., Silva, N.D., Flint, B., Frankish, A., Hunt, S.E., Ilsley, G.R., Langridge, N., Loveland, J.E., Martin, F.J., Mudge, J.M., Morales, J., Perry, E., Ruffier, M., Tate, J., Thybert, D., Trevanion, S.J., Cunningham,

F., Yates, A.D., Zerbino, D.R., Flicek, P. Ensembl 2021. Nucleic Acids Res. 2021, 49, D884-D891.

Hurley, P.C.F. and Iles, T.D. Age and growth estimation of Atlantic bluefin tuna, *Thunnus thynnus*, using otoliths. NOAA Technical Report NMFS 1983, 8, p. 71–75.

Ienaga, N., Higuchi, K., Takashi, T., Gen, K., Terayama, K. Normal hatching rate estimation for bulk samples of Pacific bluefin tuna (*Thunnus orientalis*) eggs using deep learning. Aquac. Eng. 2022, 98, 102274.

Ijiri, S., Kaneko, H., Kobayashi, T., Wang, D.-S., Sakai, F., Paul-Prasanth, B., Nakamura, M., Nagahama, Y. Sexual dimorphic expression of genes in gonads during early differentiation of a teleost fish, the Nile Tilapia *Oreochromis niloticus*. Biol. Reprod. 2008, 78, p. 333–341.

Jiang, Y., Luo, H., Hou, M., Chen, J., Tao, B., Zhu, Z., Song, Y., Hu, W. Aromatase inhibitor induces sex reversal in the protogynous hermaphroditic rice field eel (*Monopterus albus*). Aquaculture 2022, 551, 737960.

Kaneko, H., Ijiri, S., Kobayashi, T., Izumi, H., Kuramochi, Y., Wang, D.-S., Mizuno, S., Nagahama, Y. Gonadal soma-derived factor (*gsdf*), a TGF-beta superfamily gene, induces testis differentiation in the teleost fish *Oreochromis niloticus*. Mol. Cell. Endocrinol. 2015, 415, p. 87–99.

Kasala, E.R., Bodduluru, L.N., Madana, R.M., Athira, K.V., Gogoi, R., Barua, C.C.

Chemopreventive and therapeutic potential of chrysin in cancer: mechanistic perspectives. Toxicol. Lett. 2015, 233, p. 214–225.

Klüver, N., Kondo, M., Herpin, A., Mitani, H., Schartl, M. Divergent expression patterns of Sox9 duplicates in teleosts indicate a lineage specific subfunctionalization. Dev. Genes Evol. 2005, 215, p. 297–305.

Kobayashi, Y., Nagahama, Y., Nakamura, M. Diversity and plasticity of sex determination and differentiation in fishes. Sex. Dev. 2013, 7, p. 115–125.

Komatsu, T., Nakamura, S., Nakamura, M. A sex cord-like structure and some remarkable features in early gonadal sex differentiation in the marine teleost *Siganus guttatus* (Bloch). J. Fish Biol. 2006a, 68, p. 236–250.

Komatsu, T., Nakamura, S., Nakamura, M. Masculinization of female golden rabbitfish *Siganus guttatus* using an aromatase inhibitor treatment during sex differentiation. Comp. Biochem. Physiol. Part - C: Toxicol. Pharmacol. 2006b, 143, p. 402–409.

Li, M., Sun, L., Wang, D. Roles of estrogens in fish sexual plasticity and sex differentiation. Gen. Comp. Endocrinol. 2019, 277, p. 9–16.

Liu, S., Govoroun, M., D'Cotta, H., Ricordel, M.-J., Lareyre, J.-J., McMeel, O.M., Smith, T., Nagahama, Y., Guiguen, Y. Expression of cytochrome P45011β (11β-hydroxylase) gene during gonadal sex differentiation and spermatogenesis in rainbow trout, *Oncorhynchus*

mykiss. J. Steroid Biochem. Mol. Biol. 2000, 75, p. 291–298.

Love, M.I., Huber, W., Anders, S. Moderated estimation of fold change and dispersion for RNA-seq data with DESeq2. Genome Biol. 2014, 15, 550.

Lutz, C.G. Practical Genetics for Aquaculture. Blackwell Science, 2001, 256p.

Manni, M., Berkeley, M.R., Seppey, M., Zdobnov, E.M. BUSCO: Assessing genomic data quality and beyond. Curr. Protoc. 2021, 1, e323.

Masuma, S., Takebe, T., Sakakura, Y. A review of the broodstock management and larviculture of the Pacific northern bluefin tuna in Japan. Aquaculture 2011, 315, p. 2–8.

Mazaud-Guittot, S., Meugnier, E., Pesenti, S., Wu, X., Vidal, H., Gow, A., Magueresse-Battistoni, B.L. Claudin 11 deficiency in mice results in loss of the sertoli cell epithelial phenotype in the testis. Biol. Reprod. 2010, 82, p. 202–213.

Mei, J. and Gui, J.-F. Genetic basis and biotechnological manipulation of sexual dimorphism and sex determination in fish. Sci. China Life Sci. 2015, 58, p. 124–136.

Mori, T., Saito, T., Sugimoto, T., Kayaba, T. Differences on growth rate among sexes of barfin flounder (*Verasper moseri*). Sci. Rep. Hokkaido Fish. Exp. Stn. 1999, 56, p. 137–141.

Murashita, K., Hashimoto, H., Takashi, T., Eba, T., Kumon, K., Matsunari, H., Soma, S., Oku, H., Furuita, H., Yoshinaga, H., Yamamoto, T. Characterization of digestive physiology in Pacific bluefin tuna *Thunnus orientalis* juveniles fed a raw fish feed and a commercial diet.

Aquaculture 2021, 538, 736562.

Nagahama, Y., Chakraborty, T., Paul-Prasanth, B., Ohta, K., Nakamura, M. Sex determination, gonadal sex differentiation, and plasticity in vertebrate species. Physiol. Rev. 2021, 101, p. 1237–1308.

Nakamura, M., Kobayashi, T., Chang, X.-T., Nagahama, Y. Gonadal sex differentiation in teleost fish. J. Exp. Zool. 1998, 281, p. 362–372.

Nakamura, M. Morphological and physiological studies on gonadal sex differentiation in teleost fish. Aqua-BioSci. Monogr. ABSM 2013, 6, p. 1–47.

Nakamura, S., Aoki, Y., Saito, D., Kuroki, Y., Fujiyama, A., Naruse, K., Tanaka, M. *Sox9b*/*sox9a2*-EGFP transgenic medaka reveals the morphological reorganization of the gonads and a common precursor of both the female and male supporting cells. Mol. Reprod. Dev. 2008, 75, p. 472–476.

Nakamura, S., Kobayashi, K., Nishimura, T., Higashijima, S., Tanaka, M. Identification of germline stem cells in the ovary of the teleost medaka. Science 2010, 328, p. 1561–1563.

Nakamura, S., Watanabe, I., Nishimura, T., Picard, J.-Y., Toyoda, A., Taniguchi, Y., Clemente, N., Tanaka, M. Hyperproliferation of mitotically active germ cells due to defective anti-Müllerian hormone signaling mediates sex reversal in medaka. Development 2012, 139, p. 2283–2287.

Nakamura, M. Dosage-dependent changes in the effect of oral administration of methyltestosterone on gonadal sex differentiation in *Tilapia mossambica*. Fac. Fish. Hokkaido Univ. 1975, 26, p. 99–108.

Nakamura, M. and Takahashi, H. Gonadal sex differentiation in *Tilapia mossambica* with special regard to the time of estrogen treatment effective in inducing complete feminization of genetic males. Fac. Fish. Hokkaido Univ. 1973, 24, p. 1–13.

Nakamura, M., Bhandari, R.K., Higa, M. The role estrogens play in sex differentiation and sex changes of fish. Fish Physiol. Biochem. 2003, 28, p. 113–117.

Nakamura, Y., Mori, K., Saitoh, K., Oshima, K., Mekuchi, M., Sugaya, T., Shigenobu, Y., Ojima, N., Muta, S., Fujiwara, A., Yasuike, M., Oohara, I., Hirakawa, H., Chowdhury, V.S., Kobayashi, T., Nakajima, K., Sano, M., Wada, T., Tashiro, K., Ikeo, K., Hattori, M., Kuhara, S., Gojobori, T., Inouye, K. Evolutionary changes of multiple visual pigment genes in the complete genome of Pacific bluefin tuna. Proc. Natl. Acad. Sci. U.S.A. 2013, 110, p. 11061–11066.

Nakamura, Y., Higuchi, K., Kumon, K., Yasuike, M., Takashi, T., Gen, K., Fujiwara, A. Prediction of the sex-associated genomic region in tunas (*Thunnus* fishes). Int. J. Genomics 2021, 2021, 7226353.

Naylor, R. and Burke, M. Aquaculture and ocean resources: raising tigers of the sea. Annu. Rev.

Environ. Resour. 2005, 30, p. 185–218.

Negishi, M., Pedersen, L.G., Petrotchenko, E., Shevtsov, S., Gorokhov, A., Kakuta, Y., Pedersen, L.C. Structure and function of sulfotransferases. Arch. Biochem. Biophys, 2001, 390, p. 149–157.

Nishimura, T. and Tanaka, M. Gonadal development in fish. Sex. Dev. 2014, 8, p. 252–261.

Nishimura, T., Sato, T., Yamamoto, Y., Watanabe, I., Ohkawa, Y., Suyama, M., Kobayashi, S., Tanaka, M. *foxl3* is a germ cell–intrinsic factor involved in sperm-egg fate decision in medaka. Science 2015, 349, p. 328–331.

Okada, T., Honryo, T., Kawahara, M., Takahashi, I., Murayama, K., Ishibashi, Y. Appropriate size for transportation to sea cages for juvenile Pacific bluefin tuna *Thunnus orientalis* (Temminck and Schlegel). Aquac. Res. 2021, 52, p. 1282–1290.

Pandian, T.J. and Sheela, S.G. Hormonal induction of sex reversal in fish. Aquaculture 1995, 138, p. 1–22.

Piferrer, F., Beaumont, A., Falguière, J.-C., Flajšhans, M., Haffray, P., Colombo, L. Polyploid fish and shellfish: production, biology and applications to aquaculture for performance improvement and genetic containment. Aquaculture 2009, 293, 125–156.

Qin, Z., Yang, F., Tian, L., Chen, R., Xu, D., Takeuchi, Y. Induction of sex reversal in blue drum (*Nibea mitsukurii*) and gynogenetic yellow drum (*Nibea albiflora*) by oral administration

of letrozole. Aquac. Res. 2020, 51, p. 882–889.

Rahman, M.A., Arshad, A., Marimuthu, K., Ara, R., Amin, S.M.N. Inter-specific hybridization and its potential for aquaculture of fin fishes. Asian J. Anim. Vet. Adv. 2013, 8, p. 139–153.

Rajakumar, A. and Senthilkumaran, B. Steroidogenesis and its regulation in teleost-a review. Fish Physiol. Biochem. 2020, 46, p. 803–818.

Rhie, A., McCarthy, S.A., Fedrigo, O., Damas, J., Formenti, G., Koren, S., Uliano-Silva, M., Chow, W., Fungtammasan, A., Kim, J., Lee, C., Ko, B.J., Chaisson, M., Gedman, G.L., Cantin, L.J., Thibaud-Nissen, F., Haggerty, L., Bista, I., Smith, M., Haase, B., Mountcastle, J., Winkler, S., Paez, S., Howard, J., Vernes, S.C., Lama, T.M., Grutzner, F., Warren, W.C., Balakrishnan, C.N., Burt, D., George, J.M., Biegler, M.T., Iorns, D., Digby, A., Eason, D., Robertson, B., Edwards, T., Wilkinson, M., Turner, G., Meyer, A., Kautt, A.F., Franchini, P., Detrich III, H.W., Svardal, H., Wagner, M., Naylor, G.J.P., Pippel, M., Malinsky, M., Mooney, M., Simbirsky, M., Hannigan, B.T., Pesout, T., Houck, M., Misuraca, A., Kingan, S.B., Hall, R., Kronenberg, Z., Sović, I., Dunn, C., Ning, Z., Hastie, A., Lee, J., Selvaraj, S., Green, R.E., Putnam, N.H., Gut, I., Ghurye, J., Garrison, E., Sims, Y., Collins, J., Pelan, S., Torrance, J., Tracey, A., Wood, J., Dagnew, R.E., Guan, D., London, S.E., Clayton, D.F., Mello, C.V., Friedrich, S.R., Lovell, P.V., Osipova, E., Al-Ajli, F.O., Secomandi, S., Kim, H., Theofanopoulou, C., Hiller, M., Zhou, Y., Harris, R.S., Makova, K.D., Medvedev, P.,

Hoffman, J., Masterson, P., Clark, K., Martin, F., Howe, K., Flicek, P., Walenz, B.P., Kwak, W., Clawson, H., Diekhans, M., Nassar, L., Paten, B., Kraus, R.H.S., Crawford, A.J., Gilbert, M.T.P., Zhang, G., Venkatesh, B., Murphy, R.W., Koepfli, K.-P., Shapiro, B., Johnson, W.E., Palma, F.D., Marques-Bonet, T., Teeling, E.C., Warnow, T., Graves, J.M., Ryder, O.A., Haussler, D., O'Brien, S.J., Korlach, J., Lewin, H.A., Howe, K., Myers, E.W., Durbin, R., Phillippy, A.M., Jarvis, E.D. Towards complete and error-free genome assemblies of all vertebrate species. Nature 2021, 592, p. 737–746.

Roff, D.A. An allocation model of growth and reproduction in Fish. Can. J. Fish. Aquat. Sci. 1983, 40, p. 1395–1404.

Saito, D., Morinaga, C., Aoki, Y., Nakamura, S., Mitani, H., Furutani-Seiki, M., Kondoh, H., Tanaka, M. Proliferation of germ cells during gonadal sex differentiation in medaka: Insights from germ cell-depleted mutant *zenzai*. Dev. Biol. 2007, 310, p. 280–290.

Sarasquete, C., Cárdenas, S., González de Canales, ML., Pascual, E. Oogenesis in the bluefin tuna, *Thunnus thynnus* L.: A histological and histochemical study. Histol. Hisopathol. 2002, 17, p. 775–788.

Satoh, N. and Egami, N. Sex differentiation of germ cells in the teleost, *Oryzias latipes*, during normal embryonic development. J. Embryol. Exp. Morphol. 1972, 28, p. 385–395.

Sawada, Y., Kaga, T., Agawa, Y., Honryo, T., Kim, Y.-S., Nakatani, M., Okada, T., Cano, A.,

Margulies, D., Scholey, V. Growth analysis in artificially hatched Pacific bluefin tuna *Thunnus orientalis*. Aquac. Sci. 2013, 61, p. 315–319.

Sawada, Y., Okada, T., Miyashita, S., Murata, O., Kumai, H. Completion of the Pacific bluefin tuna *Thunnus orientalis* (Temminck et Schlegel) life cycle. Aquac. Res. 2005, 36, p. 413–421.

Sayers, E.W., Cavanaugh, M., Clark, K., Ostell, J., Pruitt, K.D., Karsch-Mizrachi, I. GenBank. Nucleic Acids Res. 2020, 48, D84–86.

Seoka, M., Kato, K., Kubo, T., Mukai, Y., Sakamoto, W., Kumai, H., Murata, O. Gonadal maturation of Pacific bluefin tuna *Thunnus orientalis* in captivity. Aquac. Sci. 2007, 55, p. 289–292.

Shiao, J.-C., Lu, H.-B., Hsu, J., Wang, H.-Y., Chang, S.-K., Huang, M.-Y., Ishihara, T. Changes in size, age, and sex ratio composition of Pacific bluefin tuna (*Thunnus orientalis*) on the northwestern Pacific Ocean spawning grounds. ICES J. Mar. Sci. 2017, 74, p. 204–214.

Shimose, T., Tanabe, T., Chen, K.-S., Hsu, C.-C. Age determination and growth of Pacific bluefin tuna, *Thunnus orientalis*, off Japan and Taiwan. Fish. Res. 2009, 100, p. 134–139.

Slater, G.S. and Birney, E. Automated generation of heuristics for biological sequence comparison. BMC Bioinform. 2005, 6, 31.

Strüssmann, C.A., Takashima, F., Toda, K. Sex differentiation and hormonal feminization in

pejerrey *Odontesthes bonariensis*. Aquaculture 1996, 139, p. 31–45.

Strüssmann, C.A. and Nakamura, M. Morphology, endocrinology, and environmental modulation of gonadal sex differentiation in teleost fishes. Fish Physiol. Biochem. 2002, 26, p. 13–29.

Suda, A., Nishiki, I., Iwasaki, Y., Matsuura, A., Akita, T., Suzuki, N., Fujiwara, A. Improvement of the Pacific bluefin tuna (*Thunnus orientalis*) reference genome and development of male-specific DNA markers. Sci. Rep. 2019, 9, 14450.

Uchino, T., Nakamura, Y., Sekino, M., Kai, W., Fujiwara, A., Yasuike, M., Sugaya, T., Fukuda, H., Sano, M., Sakamoto, T. Constructing genetic linkage maps using the whole genome sequence of Pacific bluefin tuna (*Thunnus orientalis*) and a comparison of chromosome structure among teleost species. Adv. Biosci. Biotechnol. 2016, 7, p. 85–122.

Vizziano, D., Randuineau, G., Baron, D., Cauty, C., Guiguen, Y. Characterization of early molecular sex differentiation in rainbow trout, *Oncorhynchus mykiss*. Dev. Dyn. 2007, 236, p. 2198–2206.

Viñas, J., Asensio, E., Cañavate, J.P., Piferrer, F. Gonadal sex differentiation in the Senegalese sole (*Solea senegalensis*) and first data on the experimental manipulation of its sex ratios. Aquaculture 2013, 384–387, p. 74–81.

Vogl, A.W., Pfeiffer, D.C., Mulholland, D., Kimel, G., Guttman, J. Unique and multifunctional adhesion junctions in the testis: Ectoplasmic specializations. Arch. Histol. Cytol. 2000, 63,

p. 1–15.

Wang, D.-S., Zhou, L.-Y., Kobayashi, T., Matsuda, M., Shibata, Y., Sakai, F., Nagahama, Y. Doublesex- and Mab-3-related transcription factor-1 repression of aromatase transcription, a possible mechanism favoring the male pathway in tilapia. Endocrinology 2010, 151, p. 1331–1340.

Webster, K.A., Schach, U., Ordaz, A., Steinfeld, J.S., Draper, B.W., Siegfried, K.R. Dmrt1 is necessary for male sexual development in zebrafish. Dev. Biol. 2017, 422, p. 33–46.

Wei, L., Li, X., Li, M., Tang, Y., Wei, J., Wang, D. Dmrt1 directly regulates the transcription of the testis-biased *Sox9b* gene in Nile tilapia (*Oreochromis niloticus*). Gene 2019, 687, p. 109–115.

Wei, L., Yang, C., Tao, W., Wang, D. Genome-wide identification and transcriptome-based expression profiling of the Sox gene family in the Nile tilapia (*Oreochromis niloticus*). Int. J. Mol. Sci. 2016, 17, 270.

Wootton, R.J. and Smith, C. Reproductive Biology of Teleost Fishes. Wiley-Blackwell, 2014, 196p.

Yamamoto, T.O. “Sex Differentiation”. Fish Physiology. Hoar, W.S. and Randall D.J. eds. New York, NY, Academic Press, 1969, p. 117–175.

Yasuda, S., Liu, C.-C., Takahashi, S., Suiko, M., Chen, L., Snow, R., Liu, M.-C. Identification

of a novel estrogen-sulfating cytosolic SULT from zebrafish: Molecular cloning, expression, characterization, and ontogeny study. Biochem. Biophys. Res. Commun. 2005, 330, p. 219–225.

Young, G., Kusakabe, M., Nakamura, I., Lokman, P.M., Goetz, F.W. “Gonadal Steroidogenesis in Teleost Fish”. Hormones and their receptors in fish reproduction. Melamed, P. and Sherwood, N. eds. Hackensack, NJ, World Scientific, 2005, p. 155–223.

Zhang, X., Guan, G., Li, M., Zhu, F., Liu, Q., Naruse, K., Herpin, A., Nagahama, Y., Li, J., Hong, Y. Autosomal *gsdf* acts as a male sex initiator in the fish medaka. Sci. Rep. 2016, 6, 19738.

Zhang, X., Li, M., Ma, H., Liu, X., Shi, H., Li, M., Wang, D. Mutation of *foxl2* or *cyp19a1a* results in female to male sex reversal in XX Nile tilapia. Endocrinology 2017, 158, p. 2634–2647.